RESEARCH ARTICLE



WILEY

A multilevel sampled-data approach for resilient navigation and control of autonomous systems

Hamidreza Jafarnejadsani¹ | Neng Wan² | Naira Hovakimyan² | Petros G. Voulgaris³

Correspondence

Hamidreza Jafarnejadsani, Department of Mechanical Engineering, Stevens Institute of Technology, Hoboken, NJ 07030. Email: hjafarne@stevens.edu

Funding information

National Science Foundation, ECCS, Grant/Award Number: 1739732; National Science Foundation, CMMI, Grant/Award Number: 1663460; Air Force Office of Scientific Research (AFOSR)

Summary

Autonomous systems are rapidly becoming an integrated part of the modern life. Safe and secure navigation and control of these systems present significant challenges in the presence of uncertainties, physical failures, and cyber attacks. In this paper, we formulate a navigation and control problem for autonomous systems using a multilevel control structure, in which the high-level reference commands are limited by a saturation function, whereas the low-level controller tracks the reference by compensating for disturbances and uncertainties. For this purpose, we consider a class of nested, uncertain, multiple-input-multiple-output systems subject to reference command saturation, possibly with nonminimum phase zeros. A multirate output-feedback \mathcal{L}_1 adaptive controller is developed as the low-level controller. The sampled-data (SD) design of this controller facilitates the direct implementation on digital computers, where the input/output signals are available at discrete time instances with different sampling rates. In addition, stealthy zero-dynamics attacks become detectable by considering a multirate SD formulation. Robust stability and performance of the overall closed-loop system with command saturation and multirate \mathcal{L}_1 adaptive control are analyzed. Simulation scenarios for navigation and control of a fixed-wing drone under failures/attacks are provided to validate the theoretical findings.

KEYWORDS

autonomous systems, cyber-physical attacks/failures, \mathcal{L}_1 adaptive control, multilevel multirate control, nested saturation, uncertain MIMO systems

1 | INTRODUCTION

The last two decades have witnessed significant progress in development of autonomous systems, including industrial/medical robots, unmanned aerial vehicles (UAVs), and self-driving cars, to name just a few. The control structures in these complex systems are often nested with multiple levels such as mission management, guidance/steering/navigation, and low-level controllers. These control loops are subject to contingencies, uncertainties, and cyber attacks from vulnerable operational environments, making it challenging to achieve trustable autonomy.

Multilevel control architectures, where a high-level controller provides reference commands to a low-level controller, are widely used for navigation and control of autonomous systems in aerospace, robotics, and many other applications. ¹⁻⁴ The main objective of multilevel control architectures is the decoupling between the outer loop and the inner loop for reliable implementation and to satisfy input/state constraints. ^{5,6} In such systems, it is desirable to limit the commands

¹Department of Mechanical Engineering, Stevens Institute of Technology, Hoboken, New Jersey

²Department of Mechanical Science and Engineering, University of Illinois at Urbana-Champaign, Urbana, Illinois

³Department of Aerospace Engineering, University of Illinois at Urbana-Champaign, Urbana, Illinois

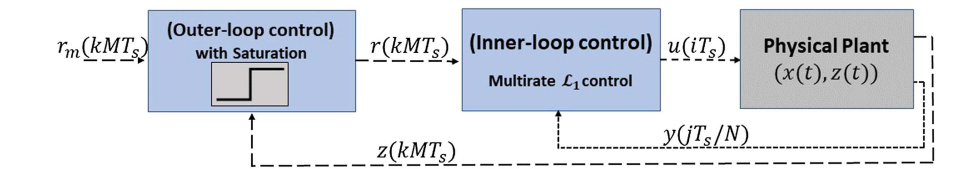
by saturation functions.⁵ Nested saturation for navigation and control of UAVs has been studied in other works.⁷⁻⁹ In the work of Teel,¹⁰ it is shown that a chain of multiple integrators can be globally stabilized using nested saturation functions. Considering a multiloop control architecture, this paper develops a sampled-data (SD) framework for navigation and control of autonomous systems. Such approach allows to analyze continuous-time physical processes that interact with digital controllers through sensors/actuators and communication links that can possibly have different sampling rates.¹¹

The SD control designs are mainly based on the controller emulation methods, where an SD controller is developed in two stages: first, a continuous-time controller is designed that satisfies certain performance/robustness requirements; next, a discrete-time controller is obtained for digital implementation using an approximation technique. ¹²⁻¹⁴ In the works of Khalil, ¹⁵ Ahrens et al, ¹⁶ and Ahmed Ali, ¹⁷ the problem of SD output-feedback control was addressed by introducing high-gain observers to estimate the unmeasured states. Output-feedback stabilization of nonlinear systems with SD controllers has been studied in the works of Shim and Teel¹⁸ and Lam. ¹⁹ Other authors ^{13,14,20-23} have addressed the problem of SD output-feedback control for systems with uncertainties and disturbances for a class of single-input-single-output nonlinear systems under a lower-triangular linear growth condition. In the works of Lin and Wei, ^{13,23} nonminimum phase nonlinear systems were considered. Nonlinear SD systems with full state-feedback were addressed in the works of Guillaume et al, ²⁴ Wu and Ding, ²⁵ and Laila et al. ²⁶

We notice that the analysis of control systems in the SD framework has also important cyber-physical security implications. The SD nature of controller implementation in autonomous systems can generate additional vulnerability to stealthy attacks due to the sampling zeros in the SD system. For example, a zero-dynamics attack can be implemented in the cyber space as an additive disturbance such that an unbounded signal can blow up the states of the physical system, while the observed output and control command dictate normal behavior. To deal with this problem, a multirate scheme is applied since it allows the attack to be detected by ensuring that there are no relevant unstable zeros in the lifted system. As shown in the work of Naghnaeian et al, unbounded zero-dynamics attacks can be detected if the control system is designed in the dual rate SD framework.

In this paper, the navigation and control problem for autonomous systems is formulated using a multirate SD control approach. The control structure consists of a high-level (outer-loop) control for reference command generation and a low-level (inner-loop) adaptive control for reference tracking, as shown in Figure 1. The high-level controller is limited by saturation bounds to maintain the closed-loop system within a safety operational envelope. The low-level controller is a multirate \mathcal{L}_1 adaptive controller for tracking the generated reference command by compensating for uncertainties and disturbances. \mathcal{L}_1 adaptive controller is a robust control technique with quantifiable performance bounds and robustness margins, 29-31 which has been successfully implemented on manned and unmanned aircraft 32-34 and simulation models. $^{35-39}$ In this paper, the \mathcal{L}_1 adaptive control theory is extended to the multirate SD framework, while maintaining the key benefits of a continuous-time \mathcal{L}_1 adaptive controller. ^{29-31,40} The low-level controller compensates for disturbances within the bandwidth of a low-pass filter, similar to other \mathcal{L}_1 adaptive controllers. Conditions are derived, under which the SD controller uniformly recovers the performance of the underlying continuous-time reference system as the sampling time tends to zero. The related preliminary results by authors can be found in the works Jafarnejadsani et al. 41,42 This paper extends the previous results, by considering the output-feedback control problem for a class nested uncertain MIMO systems subject to reference command saturation, with possibly nonminimum phase zeros. The unknown nonlinearities are assumed to be locally Lipschitz. The multirate SD framework of this paper addresses the digital implementation of the control law on computers, where the control inputs and the measurements are available at discrete time instances with different sampling rates. In addition, the multilevel structure of the problem formulation allows for design of the feedback loops for the high-level/low-level subsystems with their respective control objectives, while the stability and robustness of the overall nested system subject to command saturation are taken into account. The effectiveness of the proposed approach is evaluated using the simulation study of a fixed-wing UAV in the presence of uncertainties, zero-dynamics attack, and mechanical failure. In this example, the multilevel SD control strategy is leveraged for navigation and control of the UAV model, where the theoretical conditions for the control design are verified. The simulation environment is based on both linearized model and high-fidelity nonlinear model.

FIGURE 1 Structure of the proposed multilevel multirate sampled-data controller for navigation and control of autonomous systems [Colour figure can be viewed at wileyonlinelibrary.com]



The rest of this paper is organized as follows. A few notations and definitions are introduced in Section 2. Section 3 presents the problem formulation and the control design objectives. In Section 4, the structure of the proposed multilevel multirate controller is presented. The closed-loop SD system is analyzed in Section 5. Section 6 presents the simulation results. Finally, Section 7 concludes this paper.

2 | PRELIMINARIES

Throughout this paper, $\|x_{\tau}\|_{\mathcal{L}_{\infty}}$ denotes the \mathcal{L}_{∞} norm of the truncated signal $x_{\tau}(t)$ for the original $x(t) \in \mathbb{R}^n$, given as

$$x_{\tau}(t) = x(t), \quad \forall t \le \tau,$$

 $x_{\tau}(t) = 0_{n \times 1}, \quad \text{otherwise.}$

The notation $\|\cdot\|_p$ represents vector or matrix p-norms with $1 \le p \le \infty$. The right pseudoinverse of a full row-rank matrix $A \in \mathbb{R}^{q \times n}$ is denoted by A^{\dagger} , and can be computed as $A^{\dagger} = A^{\top} (AA^{\top})^{-1}$ such that $AA^{\dagger} = \mathbb{I}_q$. In addition, s is used for the Laplace transform. For a vector $v \in \mathbb{R}^q$, the notation sat $\{v\}$ represents the saturation function defined by

$$\operatorname{sat}\{v\} = \begin{bmatrix} \operatorname{sgn}\{v_1\} \min\{|v_1|, 1\} \\ \vdots \\ \operatorname{sgn}\{v_q\} \min\{|v_q|, 1\} \end{bmatrix}, \tag{1}$$

where $sgn\{\cdot\}$ is the standard sign function, and v_i 's are the elements of the vector v.

Consider a continuous-time LTI plant P_c , and the corresponding discrete-time LTI plant $P_d = SP_c\mathcal{H}$, which is defined with the standard zero-order hold and sample operators \mathcal{H} and \mathcal{S} , respectively. The relationship between P_c and P_d follows from the following definition.

Definition 1. For an LTI system P_c with the minimal realization (A_c, B_c, C_c, D_c) , the equivalent step-invariant discrete-time system P_d can be defined by the following state-space matrices

$$A_{\rm d} = e^{A_{\rm c}T_{\rm s}}, \quad B_{\rm d} = \int_0^{T_{\rm s}} e^{A_{\rm c}\tau} B_{\rm c} d\tau, \quad C_{\rm d} = C_{\rm c}, \quad D_{\rm d} = D_{\rm c},$$
 (2)

where $T_s > 0$ is the sampling period.

Definition 2 (Zero-dynamics attack). Assume the system P_d with the state-space matrices in (2) has an unstable transmission zero at $a_0 \in \mathbb{C}$. Then, the unbounded actuator attack signal of the form $d[k] = \epsilon a_0^k$, which implemented as an additive input disturbance, can cause the states of the system expand exponentially, while remaining undetected for small enough ϵ at the sampled output.²⁸

3 | PROBLEM FORMULATION

As depicted in Figure 1, consider the following multilevel model for an autonomous system subject to uncertainties, disturbances, physical faults, and attack signals, comprised of a low-level (inner-loop) subsystem

$$\dot{x}(t) = A_{x}x(t) + B_{x}(u(t) + f(t, x(t)) + d(t)), \ x(0) = x_{0},$$

$$y(t) = C_{x}x(t),$$
(3)

and a high-level (outer-loop) subsystem

$$\dot{z}(t) = A_z z(t) + B_z y(t) + g(t, x(t)), \quad z(0) = z_0,$$
(4)

where $x(t) \in \mathbb{R}^n$ and $z(t) \in \mathbb{R}^p$ are the state vectors, $u(t) \in \mathbb{R}^q$ is the input signal, and $y(t) \in \mathbb{R}^q$ is the system output vector. In addition, $\{A_x \in \mathbb{R}^{n \times n}, B_x \in \mathbb{R}^{n \times q}, C_x \in \mathbb{R}^{q \times n}\}$ is an observable-controllable triple and $\{A_z \in \mathbb{R}^{p \times p}, B_z \in \mathbb{R}^{p \times q}\}$

is a controllable pair. The unknown initial condition $x_0 \in \mathbb{R}^n$ is assumed to be inside an arbitrarily large set, so that $\|x_0\|_{\infty} \leq \rho_0 < \infty$ for some known $\rho_0 > 0$, and $z_0 \in \mathbb{R}^p$ is a known initial condition. Let $d(t) \in \mathbb{R}^q$ be an exogenous additive disturbance on the control input, which can represent a CPS attack (eg, stealthy zero-dynamics attack signal) or failure. In addition, let $f(t, x(t)) \in \mathbb{R}^q$ and $g(t, x(t)) \in \mathbb{R}^p$ represent the time-varying uncertainties and disturbances, subject to the following assumption.

Assumption 1. There exist $K_{\delta} > 0$ and $G_{\delta} > 0$ for arbitrary $\delta > 0$, and constants $L_0 > 0$ and $L_1 > 0$ such that

$$||f(t,x_2) - f(t,x_1)||_{\infty} \le K_{\delta} ||x_2 - x_1||_{\infty}, \quad ||f(t,0)||_{\infty} \le L_0, \quad ||d(t)||_{\infty} \le L_1, \quad ||g(t,x_1)||_{\infty} \le G_{\delta}$$

hold for all $||x_i||_{\infty} \le \delta$, $i \in \{1, 2\}$, uniformly in $t \ge 0$.

Using a multirate SD control approach, the control input and the measurements are available at discrete time instances with different sampling periods. The control input, which is implemented via a zero-order hold mechanism with time period of $T_s > 0$, is given by

$$u(t) = u_{\rm d}[i], \quad t \in [iT_{\rm s}, (i+1)T_{\rm s}), \quad i \in \mathbb{Z}_{>0},$$
 (5)

where $u_d[i]$ is a discrete-time control input signal. The output of the low-level subsystem y(t) is sampled $N \in \mathbb{N}$ times faster with the sampling time of T_s/N , such that the discrete-time output signal $y_d[j]$ is given by

$$y_{\mathbf{d}}[j] = y\left(j\frac{T_{\mathbf{s}}}{N}\right), \quad t \in \left[j\frac{T_{\mathbf{s}}}{N}, (j+1)\frac{T_{\mathbf{s}}}{N}\right), \quad j \in \mathbb{Z}_{\geq 0},$$
 (6)

and the high-level subsystem state z(t) is sampled $M \in \mathbb{N}$ times slower with the period of MT_s such that

$$z_{\mathbf{d}}[k] = z(kMT_{\mathbf{s}}), \quad t \in [kMT_{\mathbf{s}}, (k+1)MT_{\mathbf{s}}), \quad k \in \mathbb{Z}_{>0}. \tag{7}$$

For M = N = 1, the SD controller will have a uniform rate. In the more general case where the inputs and outputs are available at different rates, $N, M \in \mathbb{N}$ can be selected as desired for the control structure accordingly.

Remark 1. The proposed multirate control structure is motivated by real-world applications. In navigation and control of autonomous UAVs as an example, the attitude angles for inner-loop dynamics are measured at the rate of 50 Hz or faster using inertial measurement unit (IMU) sensor, while the position measurement for the outer-loop dynamics is available at the slower sampling rate of about 10 Hz using global positioning system (GPS) sensor. In addition, the multirate sampling approach has the advantage of improving the detectability of zero-dynamics attacks.²⁸

Assumption 2. The desired dynamics for the low-level subsystem in (3) is defined by

$$P_{\rm m}(s) = C_{\rm m} (s \mathbb{I}_{n_{\rm m}} - A_{\rm m})^{-1} B_{\rm m}, \tag{8}$$

where the triple $\{A_{\rm m} \in \mathbb{R}^{n_{\rm m} \times n_{\rm m}}, B_{\rm m} \in \mathbb{R}^{n_{\rm m} \times q}, C_{\rm m} \in \mathbb{R}^{q \times n_{\rm m}}\}$ is a minimal state-space realization of $P_{\rm m}(s)$, with $A_{\rm m}$ being Hurwitz, and $(C_{\rm m}B_{\rm m})$ is nonsingular. In addition, $P_{\rm m}(s)$ does not have any unstable transmission zeros.

The desired response $y_m(t)$ is given by the Laplace transform $y_m(s) = P_m(s)K_gr(s)$, where

$$K_{\rm g} \stackrel{\Delta}{=} - (C_{\rm m} A_{\rm m}^{-1} B_{\rm m})^{-1},$$

and r(s) is the Laplace transform of r(t) given by

$$r(t) = r_{\rm d}[k], \quad t \in \left[kMT_{\rm s}, (k+1)MT_{\rm s}\right), \quad k \in \mathbb{Z}_{\geq 0},\tag{9}$$

where $r_d[k]$ is a discrete-time reference command.

Assumption 3. The reference command is constrained to a convex polytope as a safe operation region, defined by the set

$$\mathcal{R} = \left\{ r \in \mathbb{R}^q | \|Wr\|_{\infty} \le 1 \right\},\tag{10}$$



where $W = \text{diag}\{r_{\max_i}^{-1}, \dots, r_{\max_q}^{-1}\}$, and the positive constants r_{\max_i} 's are the saturation bounds on control inputs. Then, the weighted reference command is bounded by

$$||Wr_{\mathsf{d}}[k]||_{\infty} \leq 1, \quad k \in \mathbb{Z}_{>0}.$$

Remark 2. For large uncertainties outside normal conditions, the low-level control inputs can saturate or drive the system to unsafe states. By restricting the reference commands (generated by high-level control) to a safe operational envelope, as defined in Assumption 3, the safety of the autonomous system can be improved.

Assumption 4. The desired system for the high-level subsystem in (4) is defined by

$$\dot{z}_{\rm m}(t) = A_{\rm z} z_{\rm m}(t) + B_{\rm z} r_{\rm m}(t), \quad z_{\rm m}(0) = z_0,$$
 (11)

where $z_{\rm m}(t) \in \mathbb{R}^p$ is the desired state for the high-level subsystem, and

$$r_{\mathbf{m}}(t) = r_{\mathbf{m}_{\mathbf{d}}}[k], \quad t \in \left[kMT_{\mathbf{s}}, (k+1)MT_{\mathbf{s}}\right), \quad k \in \mathbb{Z}_{\geq 0}$$

$$\tag{12}$$

is the precalculated reference command for the desired system. It is assumed that

$$||Wr_{\mathbf{m}_{d}}[k]||_{\mathfrak{m}} \le \alpha, \quad k \in \mathbb{Z}_{\ge 0},\tag{13}$$

where $\alpha \in (0, 1)$ is a given constant, and W is defined in (10). In addition, we assume that $r_{m_d}[0] = 0$, and

$$\frac{1}{MT_{s}} \| r_{m_{d}}[k+1] - r_{m_{d}}[k] \|_{\infty} \le \delta_{r_{m}}, \quad k \in \mathbb{Z}_{\ge 0},$$
(14)

where $\delta_{r_m} > 0$ is the bound on the rate of change of the reference command.

In the following, a multilevel multirate adaptive controller is formulated to:

- compensate for physical failures, uncertainties, and disturbances, such that the low-level system in (3) is stable and the output y(t) closely tracks the desired response $y_m(t)$;
- maintain the reference command r(t) within the safe operation envelope \mathcal{R} defined in (10);
- bound the error between the states of the high-level subsystem, z(t), and the desired trajectory $z_m(t)$ given in (11);
- detect sensor/actuator attacks (including stealthy zero-dynamics attacks), and recover stability of the perturbed system.

4 | PROPOSED MULTILEVEL MULTIRATE CONTROLLER

In this section, the proposed multilevel multirate controller is presented. The conditions for selection of the control parameters and the detailed analysis of the closed-loop system are provided in Section 5. First, the elements of the multirate output-feedback \mathcal{L}_1 adaptive controller that generates the input u(t) to the low-level subsystem in (3) are given.

Let $T_s > 0$ be the sampling time of the control input. Consider a strictly proper stable transfer function C(s) such that $C(0) = \mathbb{I}_q$. In the \mathcal{L}_1 adaptive control structure, C(s) represents the low-pass filter at the control input.³⁰ In addition, define $O(s) \stackrel{\Delta}{=} C(s) P_{\mathrm{m}}^{-1}(s) C_{\mathrm{m}} \left(s \mathbb{I}_{n_{\mathrm{m}}} - A_{\mathrm{m}} \right)^{-1}$, and let $\{A_0 \in \mathbb{R}^{\nu \times \nu}, B_0 \in \mathbb{R}^{\nu \times q}, C_0 \in \mathbb{R}^{q \times \nu}\}$ be a minimal state-space realization such that

$$C_0(s\mathbb{I}_v - A_0)^{-1}B_0 = O(s). (15)$$

The control laws are given by

$$x_{\mathbf{u}}[j+1] = e^{A_{0}\frac{T_{\mathbf{s}}}{N}}x_{\mathbf{u}}[j] + A_{0}^{-1}\left(e^{A_{0}\frac{T_{\mathbf{s}}}{N}} - \mathbb{I}_{v}\right)B_{0}e^{-A_{\mathbf{m}}\frac{T_{\mathbf{s}}}{N}}\hat{\sigma}_{\mathbf{d}}[j], \quad x_{\mathbf{u}}[0] = 0, \quad j \in \mathbb{Z}_{\geq 0},$$

$$u_{\mathbf{N}_{\mathbf{d}}}[j] = -C_{0}x_{\mathbf{u}}[j],$$

$$u_{\mathbf{N}}(t) = u_{\mathbf{N}_{\mathbf{d}}}[j], \quad t \in \left[j\frac{T_{\mathbf{s}}}{N}, (j+1)\frac{T_{\mathbf{s}}}{N}\right),$$

$$u_{\mathbf{d}}[i] = u_{\mathbf{N}}(iT_{\mathbf{s}}) + K_{\mathbf{g}}r(iT_{\mathbf{s}}), \quad i \in \mathbb{Z}_{\geq 0},$$

$$(16)$$

where $\hat{\sigma}_{d}[\cdot] \in \mathbb{R}^{n}$ is provided by the adaptation law in (22). In addition, the reference command $r(\cdot) \in \mathbb{R}^{q}$ is given by (9) and the high-level controller in (24).

The construction of $\hat{\sigma}_d[\cdot]$ is based on an output predictor that follows. The output predictor is given by

$$\hat{x}_{d}[j+1] = e^{A_{m} \frac{T_{s}}{N}} \hat{x}_{d}[j] + A_{m}^{-1} \left(e^{A_{m} \frac{T_{s}}{N}} - \mathbb{I}_{n_{m}} \right) (B_{m} u_{P}[j] + \hat{\sigma}_{d}[j]), \quad \hat{x}_{d}[0] = C_{m}^{\dagger} y_{0}, \quad j \in \mathbb{Z}_{\geq 0},$$

$$\hat{y}_{d}[j] = C_{m} \hat{x}_{d}[j].$$
(17)

The predictor control input $u_P[j]$ is defined by

$$u_{\mathbf{P}}[j] = u\left(j\frac{T_{\mathbf{S}}}{N}\right), \quad j \in \mathbb{Z}_{\geq 0},$$
 (18)

where u(t) is defined by (5) and (16).

Given that $A_{\rm m} \in \mathbb{R}^{n_{\rm m} \times n_{\rm m}}$ is Hurwitz, there exists a positive definite matrix $P \in \mathbb{R}^{n_{\rm m} \times n_{\rm m}}$ solving $A_{\rm m}^\top P + P A_{\rm m} = -Q$ for a given positive definite matrix $Q \in \mathbb{R}^{n_{\rm m} \times n_{\rm m}}$. Define

$$\Lambda \stackrel{\Delta}{=} \begin{bmatrix} C_{\rm m} \\ D\sqrt{P} \end{bmatrix},\tag{19}$$

where \sqrt{P} satisfies $P = \sqrt{P}^{\top} \sqrt{P}$, and $D \in \mathbb{R}^{(n_{\rm m}-q)\times n_{\rm m}}$ is a matrix that is in the null space of $C_{\rm m}(\sqrt{P})^{-1}$, ie,

$$D\left(C_{\rm m}\left(\sqrt{P}\right)^{-1}\right)^{\rm T}=0. \tag{20}$$

Furthermore, let $\Phi(\cdot)$ be the $n_{\rm m} \times n_{\rm m}$ matrix

$$\Phi(T_{\rm s}) \stackrel{\Delta}{=} \int_0^{\frac{T_{\rm s}}{N}} e^{\Lambda A_{\rm m} \Lambda^{-1} \left(\frac{T_{\rm s}}{N} - \tau\right)} \Lambda d\tau. \tag{21}$$

The adaptation law is governed by the following equation:

$$\hat{\sigma}_{d}[j] = -\Phi^{-1}(T_{s}) e^{\Lambda A_{m} \Lambda^{-1} \frac{T_{s}}{N}} \mathbf{1}_{n, q} \tilde{y}_{d}[j], \quad j \in \mathbb{Z}_{>0}, \tag{22}$$

where $\tilde{y}_d[j] = \hat{y}_d[j] - y_d[j]$, and $\mathbf{1}_{n_m q} \in \mathbb{R}^{n_m \times q}$ is given by

$$\mathbf{1}_{n_{\mathbf{m}}q} \stackrel{\triangle}{=} \begin{bmatrix} \mathbb{I}_q \\ 0_{(n_{\mathbf{m}}-q)\times q} \end{bmatrix} . \tag{23}$$

Finally, the reference command $r_d[k]$, which is generated by the high-level control law, is given by

$$r_{\rm d}[k] = r_{\rm m_d}[k] + (1 - \alpha)W^{-1} \operatorname{sat} \left\{ \frac{1}{1 - \alpha} W F_{\rm z} \left(z_{\rm m_d}[k] - z_{\rm d}[k] \right) \right\}, \quad k \in \mathbb{Z}_{\geq 0}, \tag{24}$$

where $r_{m_d}[k]$ is the desired reference command introduced in Assumption 4, and $F_z \in \mathbb{R}^{q \times p}$ is the state-feedback gain, while α is introduced in Assumption 4. In addition, $z_d[k]$ is the measured high-level state given by (4) and (7). Using (11), the desired high-level state $z_{m_a}[k]$ is obtained by

$$z_{\mathbf{m}_{d}}[0] = z_{0},$$

$$z_{\mathbf{m}_{d}}[k] = e^{A_{z}(kMT_{s})}z_{0} + \sum_{l=0}^{k-1} \left(\int_{0}^{MT_{s}} e^{A_{z}((k-l)MT_{s}-\tau)} B_{z} d\tau \right) r_{\mathbf{m}_{d}}[l], \quad k \in \mathbb{Z}_{>0}.$$
(25)

Notice that the saturation function in (24) ensures that the reference command always remains within the safety envelope \mathcal{R} defined in (10). In the ideal case where the outer-loop state z(t) precisely tracks the desired state $z_{\rm m}(t)$, the reference command law in (24) implies that $r(t) = r_{\rm m}(t)$. While r(t) represents the command that is sent to the inner-loop subsystem, $r_{\rm m}(t)$ is the precalculated reference command for the desired system in (11) with no uncertainty.

5 | ANALYSIS OF THE CLOSED-LOOP MULTIRATE SYSTEM

This section provides the analysis of stability and performance of the closed-loop SD system with the proposed controller. In addition, the conditions for selection of the control parameters T_s , C(s), and F_z are provided. The analysis is summarized in Theorems 1 and 2 at the end of this section. Toward this goal, we need to define a few variables of interest and design constraints. Let

$$P(s) \stackrel{\Delta}{=} C_{X}(s\mathbb{I}_{n} - A_{X} + B_{X}F_{X})^{-1}B_{X},$$

$$H_{0}(s) \stackrel{\Delta}{=} (s\mathbb{I}_{n} - A_{X} + B_{X}F_{X})^{-1}B_{X},$$

$$H_{1}(s) \stackrel{\Delta}{=} (\mathbb{I}_{q} + (P_{m}^{-1}(s)P(s) - \mathbb{I}_{q}) C(s))^{-1},$$

$$H_{2}(s) \stackrel{\Delta}{=} H_{0}(s) - H_{0}(s)C(s)H_{1}(s) (P_{m}^{-1}(s)P(s) - \mathbb{I}_{q}),$$

$$H_{3}(s) \stackrel{\Delta}{=} H_{1}(s)P_{m}^{-1}(s)P(s),$$

$$H_{4}(s) \stackrel{\Delta}{=} H_{1}(s) (P_{m}^{-1}(s)P(s) - \mathbb{I}_{q}),$$

$$H_{5}(s) \stackrel{\Delta}{=} H_{0}(s)C(s)H_{1}(s)P_{m}^{-1}(s),$$

$$G(s) \stackrel{\Delta}{=} H_{0}(s) - H_{5}(s)P(s),$$

$$(26)$$

where $F_x \in \mathbb{R}^{q \times n}$ is selected such that $A_x - B_x F_x$ is Hurwitz. Let $y_0 \stackrel{\Delta}{=} C_x x_0$ be the known initial output. Define the auxiliary system

$$\dot{x}_{a}(t) = A_{m}x_{a}(t) + B_{m}(u(t) + \sigma(t)), \quad x_{a}(0) = C_{m}^{\dagger}y_{0},
y(t) = C_{m}x_{a}(t),$$
(27)

with the same input u(t) to output y(t) mapping as the system in (3), where $x_a(t) \in \mathbb{R}^{n_m}$ is the state vector, and the Laplace transform of $\sigma(t)$ is given by

$$\sigma(s) = P_{\rm m}^{-1}(s) \left((P(s) - P_{\rm m}(s)) u(s) + P(s)w(s) + H_{\rm in}(s)x_0 \right),\,$$

where

$$H_{\text{in}}(s) \stackrel{\Delta}{=} C_{\text{x}}(s\mathbb{I}_n - A_{\text{x}} + B_{\text{x}}F_{\text{x}})^{-1} - C_{\text{m}}(s\mathbb{I}_{n_{\text{m}}} - A_{\text{m}})^{-1}C_{\text{m}}^{\dagger}C_{\text{x}},$$

and w(s) is the Laplace transform of w(t) given by

$$w(t) = F_{x}x(t) + f(t, x(t)) + d(t).$$
(28)

The term $\sigma(t)$ in (27), which appears as a matched signal in the input channel, lumps together the uncertainties originated from (i) the model mismatch between the given and desired system dynamics, (ii) uncertainty terms f(t, x(t)) and d(t), and (iii) unknown initial condition. The design objective is to recover the desired system response by partially compensating

for $\sigma(t)$ using the control input u(t). In practice, complete cancelation of the uncertainty $\sigma(t)$ can be achieved only in the expense of losing robustness. For a robust design, the controller compensates for $\sigma(t)$ within the bandwidth of a low-pass filter in this paper.

Remark 3. Assumption 2 implies that $\frac{1}{s}P_{\rm m}^{-1}(s)$ is a proper transfer function. Given that $P_{\rm m}(s)$ does not have an unstable transmission zero, $P_{\rm m}^{-1}(s)P(s)$ is proper and stable, and $P_{\rm m}^{-1}(s)H_{\rm in}(s)$ is strictly proper and stable ($H_{\rm in}(s)$ has total relative degree of two or higher). Therefore, $\sigma(t)$ in (27) is a causal signal. In addition, Assumption 1 states that the signals f(t, x(t)) and d(t) are uniformly bounded with respect to time and f(t, x(t)) is locally Lipschitz continuous with respect to x(t). Therefore, the Laplace transform of w(t) in (28) exists.

Furthermore, for every $\delta > 0$, let

$$L_{\delta} \stackrel{\Delta}{=} \frac{\bar{\gamma}_1 + \delta}{\delta} \left(K_{(\bar{\gamma}_1 + \delta)} + \|F_{\mathbf{x}}\|_{\infty} \right), \tag{29}$$

where K_{δ} is introduced in Assumption 1, and $\bar{\gamma}_1$ is an arbitrarily small positive constant. It can be shown that the following bound on w(t) holds:

$$||w_t||_{\mathcal{L}_m} \le L_\delta ||x_t||_{\mathcal{L}_m} + L_2,\tag{30}$$

where $L_2 \stackrel{\Delta}{=} L_0 + L_1$. In addition, define

$$M_{\rm r} \stackrel{\Delta}{=} \max \left\{ r_{\max_1}, \dots, r_{\max_n} \right\},\tag{31}$$

where r_{\max_i} 's are introduced in (10). The design of the controller proceeds by finding a low-pass filter C(s) such that $C(0) = \mathbb{I}_q$. The selection of C(s) must ensure that

$$H_1(s)$$
 is stable, (32)

where $H_1(s)$ is defined in (26), and for a given ρ_0 , there exists $\rho_r > \rho_0$ such that the following \mathcal{L}_1 -norm condition holds:

$$||G(s)||_{\mathcal{L}_1} < \frac{\rho_r - \rho_1 - \rho_2}{L_{\rho_r}\rho_r + L_2},$$
 (33)

where

$$\rho_1 \stackrel{\triangle}{=} \| s(s\mathbb{I}_n - A_x + B_x F_x)^{-1} - sH_5(s)H_{\text{in}}(s) \|_{\mathcal{L}_1} \rho_0, \quad \rho_2 \stackrel{\triangle}{=} \| H_2(s)K_g \|_{\mathcal{L}_1} M_r.$$
 (34)

Remark 4. Selection of the filter C(s) provides a trade-off between performance in terms of disturbance compensation and robustness in terms of input-delay margin. A mixed-norm optimization of the filter for \mathcal{L}_1 adaptive control structure can be found in the work of Jafarnejadsani et al.³⁸

In the following, we define a few more variables required to obtain the conditions for selection of the sampling time T_s for the digital controller. Let $P_1 \in \mathbb{R}^{q \times q}$ and $P_2 \in \mathbb{R}^{(n_m-q)\times (n_m-q)}$ be positive definite matrices given by

$$P_1 \stackrel{\Delta}{=} \left(C_{\rm m} \sqrt{P}^{-1} \sqrt{P}^{-T} C_{\rm m}^{\mathsf{T}} \right)^{-1}, \quad P_2 \stackrel{\Delta}{=} (DD^{\mathsf{T}})^{-1}.$$
 (35)

Define

$$\left[\eta_1^{\mathsf{T}}(t) \quad \eta_2^{\mathsf{T}}(t)\right] \stackrel{\Delta}{=} \mathbf{1}_{n_{\mathrm{m}}q}^{\mathsf{T}} e^{\Lambda A_{\mathrm{m}} \Lambda^{-1} t},\tag{36}$$

where $\eta_1(t) \in \mathbb{R}^{q \times q}$ and $\eta_2(t) \in \mathbb{R}^{(n_{\rm m}-q) \times q}$, and

$$\kappa(T_{\rm S}) \stackrel{\Delta}{=} \int_0^{\frac{T_{\rm S}}{N}} \left\| \mathbf{1}_{n_{\rm m}q}^{\top} e^{\Lambda A_{\rm m} \Lambda^{-1} \left(\frac{T_{\rm S}}{N} - \tau \right)} \Lambda B_{\rm m} \right\|_2 d\tau. \tag{37}$$

Define the function

$$\Gamma(T_{s}) \stackrel{\Delta}{=} \alpha_{1}(T_{s}) \left\| (s \mathbb{I}_{v} - A_{o})^{-1} B_{o} \right\|_{\mathcal{L}_{1}} + \alpha_{2}(T_{s}), \tag{38}$$

where the system matrices (A_0, B_0, C_0) satisfy (15), and

$$\alpha_1(T_{\mathrm{S}}) \stackrel{\Delta}{=} \max_{t \in \left[0, \frac{T_{\mathrm{S}}}{N}\right]} \left\| C_{\mathrm{O}} \left(e^{A_{\mathrm{o}}t} - \mathbb{I}_{v} \right) \right\|_{\infty}, \quad \alpha_2(T_{\mathrm{S}}) \stackrel{\Delta}{=} \max_{t \in \left[0, \frac{T_{\mathrm{S}}}{N}\right]} \int_{0}^{t} \left\| C_{\mathrm{o}} e^{A_{\mathrm{o}}(t-\tau)} B_{\mathrm{o}} \right\|_{\infty} d\tau.$$

Let

$$\Upsilon(T_{s}) = \left\| e^{-A_{m} \frac{T_{s}}{N}} \Phi^{-1}(T_{s}) e^{\Lambda A_{m} \Lambda^{-1} \frac{T_{s}}{N}} \mathbf{1}_{n_{m}q} \right\|_{\infty},
\Psi(T_{s}) = \left\| H_{5}(s) C_{m} \left(s \mathbb{I}_{n_{m}} - A_{m} \right)^{-1} \left(e^{A_{m} \frac{T_{s}}{N}} - \mathbb{I}_{n_{m}} \right) \right\|_{\mathcal{L}_{1}},
\Omega_{1}(T_{s}) = \left(1 - \| G(s) \|_{\mathcal{L}_{1}} L_{\rho_{r}} \right)^{-1} \| H_{2}(s) C(s) P_{m}^{-1}(s) \|_{\mathcal{L}_{1}} + \| H_{2}(s) \|_{\mathcal{L}_{1}} \left(1 - \| G(s) \|_{\mathcal{L}_{1}} L_{\rho_{r}} \right)^{-1} (N\Gamma(T_{s}) + \Psi(T_{s})) \Upsilon(T_{s}),
\rho_{\Delta} = \| H_{3}(s) \|_{\mathcal{L}_{1}} \left(L_{\rho_{r}} \rho_{r} + L_{2} \right) + \| H_{4}(s) K_{g} \|_{\mathcal{L}_{1}} M_{r} + \| s H_{1}(s) P_{m}^{-1}(s) H_{\text{in}}(s) \|_{\mathcal{L}_{1}} \rho_{0},$$
(39)

where $H_i(\cdot)$'s are defined in (26). Next, we introduce the functions

$$\beta_1(T_s) \stackrel{\Delta}{=} \max_{t \in \left[0, \frac{T_s}{N}\right]} \|\eta_1(t)\|_2, \quad \beta_2(T_s) \stackrel{\Delta}{=} \max_{t \in \left[0, \frac{T_s}{N}\right]} \|\eta_2(t)\|_2, \tag{40}$$

where $\eta_1(t)$ and $\eta_2(t)$ are given in (36). In addition,

$$\beta_3(T_s) \stackrel{\Delta}{=} \max_{t \in \left[0, \frac{T_s}{N}\right]} \eta_3(t, T_s), \quad \beta_4(T_s) \stackrel{\Delta}{=} \max_{t \in \left[0, \frac{T_s}{N}\right]} \eta_4(t), \tag{41}$$

where

$$\eta_{3}(t, T_{s}) \stackrel{\Delta}{=} \int_{0}^{t} \left\| \mathbf{1}_{n_{m}q}^{\mathsf{T}} e^{\Lambda A_{m}\Lambda^{-1}(t-\tau)} \Lambda \Phi^{-1}(T_{s}) e^{\Lambda A_{m}\Lambda^{-1}\frac{T_{s}}{N}} \mathbf{1}_{n_{m}q} \right\|_{2} d\tau, \quad \eta_{4}(t) \stackrel{\Delta}{=} \int_{0}^{t} \left\| \mathbf{1}_{n_{m}q}^{\mathsf{T}} e^{\Lambda A_{m}\Lambda^{-1}(t-\tau)} \Lambda B_{m} \right\|_{2} d\tau.$$

$$(42)$$

For $\bar{\gamma}_0 > 0$, let

$$\Delta_{1}(\bar{\gamma}_{0}) \stackrel{\Delta}{=} \rho_{\Delta} + \left(\|H_{3}(s)\|_{\mathcal{L}_{1}} L_{\rho_{r}} \Omega_{1}(T_{s}) + \|H_{4}(s)C(s)P_{m}^{-1}(s)\|_{\mathcal{L}_{1}} + \|H_{4}(s)\|_{\mathcal{L}_{1}} (N\Gamma(T_{s}) + \Psi(T_{s})) \Upsilon(T_{s}) \right) \bar{\gamma}_{0},$$

$$\Delta_{2}(\bar{\gamma}_{0}) \stackrel{\Delta}{=} \lambda_{\max} \left(\Lambda^{-\top} P \Lambda^{-1} \right) \left(\frac{2\sqrt{q} \Delta_{1}(\bar{\gamma}_{0}) \|\Lambda^{-\top} P B_{m}\|_{2}}{\lambda_{\min} \left(\Lambda^{-\top} Q \Lambda^{-1} \right)} \right)^{2},$$
(43)

where ρ_{Δ} is defined in (39). In addition, let

$$\varsigma(\bar{\gamma}_0, T_s) \stackrel{\Delta}{=} \left\| \eta_2 \left(\frac{T_s}{N} \right) \right\|_2 \sqrt{\frac{\Delta_2(\bar{\gamma}_0)}{\lambda_{\max}(P_2)}} + \sqrt{q} \kappa(T_s) \Delta_1(\bar{\gamma}_0), \tag{44}$$

where $\eta_2(\cdot)$ is defined in (36) and $\kappa(\cdot)$ is given in (37). Let

$$\gamma_0(\bar{\gamma}_0, T_s) \stackrel{\Delta}{=} \beta_1(T_s) \varsigma(\bar{\gamma}_0, T_s) + \beta_2(T_s) \sqrt{\frac{\Delta_2(\bar{\gamma}_0)}{\lambda_{\max}(P_2)}} + \beta_3(T_s) \varsigma(\bar{\gamma}_0, T_s) + \sqrt{q} \beta_4(T_s) \Delta_1(\bar{\gamma}_0). \tag{45}$$

Let μ be a positive constant, and $T_{s_{max}} > 0$ be a given upper bound on the sampling time T_s . For $F_z \in \mathbb{R}^{q \times p}$, define

$$\Delta_{s}(\mu, F_{z}) \stackrel{\triangle}{=} \frac{\|B_{z}\|_{\infty}}{\mu} M_{r} \|WF_{z}\|_{\infty} v_{1},$$

$$\Delta_{F}(\mu, F_{z}) \stackrel{\triangle}{=} \|B_{z}\|_{\infty} \|P_{m}(s)(\mathbb{I}_{q} - C(s))\|_{\mathcal{L}_{1}} \rho_{\Delta} + \|B_{z}\|_{\infty} \|C_{x}\|_{\infty} \bar{\gamma}_{1} + \bar{\gamma}_{r} + G_{\rho_{r} + \bar{\gamma}_{1}} + \|B_{z}\|_{\infty} \left\|\frac{\mu}{s + \mu} \mathbb{I}_{q} - P_{m}(s)K_{g}\right\|_{\mathcal{L}_{1}} M_{r}$$

$$+ \|B_{z}\|_{\infty} \left\|sC_{m}(s\mathbb{I}_{q} - A_{m})^{-1}C_{m}^{\dagger}C_{m}\right\|_{\mathcal{L}_{1}} \rho_{0} + \frac{\|B_{z}\|_{\infty}}{\mu} \left(\delta_{r_{m}} + M_{r}\|WF_{z}\|_{\infty}G_{\rho_{r} + \bar{\gamma}_{1}} v_{2}\right)$$

$$+ \frac{M_{r}}{\mu} \|B_{z}\|_{\infty}^{2} \|WF_{z}\|_{\infty} (\alpha M_{r} + \|C_{x}\|_{\infty}(\rho_{r} + \bar{\gamma}_{1})) v_{2},$$
(46)

where $\bar{\gamma}_r$ is an arbitrarily small positive constant, and

$$v_{1} \stackrel{\Delta}{=} \sup_{t \in (0, MT_{\text{Smax}})} \frac{1}{t} \| e^{A_{z}t} - \mathbb{I}_{p} \|_{\infty}, \quad v_{2} \stackrel{\Delta}{=} \sup_{t \in (0, MT_{\text{Smax}})} \frac{1}{t} \int_{0}^{t} \| e^{A_{z}(t-\tau)} \|_{\infty} d\tau.$$
 (47)

Following a notation similar to the work of Fang et al,⁴³ let \mathcal{D} be the set of $q \times q$ diagonal matrices whose diagonal elements are either 1 or 0. There are 2^q elements in \mathcal{D} , and we denote its elements as D_i , $i \in \{1, \ldots, 2^q\}$. Denote $D_i^- = \mathbb{I}_q - D_i$. It is easy to see that $D_i^- \in \mathcal{D}$. Let the positive definite matrix $S \in \mathbb{R}^{p \times p}$ be given. Next, the high-level controller design proceeds by considering F_z , $H_z \in \mathbb{R}^{q \times p}$, a positive definite $R \in \mathbb{R}^{p \times p}$, and a constant $\mu > 0$ such that

$$(A_{z} - B_{z} (D_{i}F_{z} + D_{i}^{-}H_{z}))^{\mathsf{T}}R + R (A_{z} - B_{z} (D_{i}F_{z} + D_{i}^{-}H_{z})) + S < 0_{p \times p}, \quad \forall i \in \{1, \dots, 2^{q}\},$$

$$(48)$$

and

$$\|WH_{z}\|_{\infty} \le (1-\alpha)\rho_{z}^{-1},$$
 (49)

where α is introduced in Assumption 4, and

$$\rho_{z} = \left(1 - \frac{2\sqrt{p}\|R\|_{2}\Delta_{s}(\mu, F_{z})}{\lambda_{\min}(S)}\right)^{-1} \frac{2\sqrt{p}\|R\|_{2}\Delta_{F}(\mu, F_{z})}{\lambda_{\min}(S)},\tag{50}$$

with $\Delta_s(\mu, F_z)$ and $\Delta_F(\mu, F_z)$ defined in (46).

Finally, define

$$\gamma_{z}(\bar{\gamma}_{0}, T_{s}) \stackrel{\Delta}{=} \alpha_{3}(T_{s})\rho_{z} + \alpha_{4}(T_{s}) \left(\|B_{z}\|_{\infty} \left(\alpha M_{r} + \|C_{x}\|_{\infty} (\rho_{r} + \Omega_{1}(T_{s})\bar{\gamma}_{0}) \right) + G_{\rho_{r} + \bar{\gamma}_{1}} \right),
\gamma_{r}(\bar{\gamma}_{0}, T_{s}) \stackrel{\Delta}{=} \|B_{z}\|_{\infty} M_{r} \left(2(1 - e^{-\mu M T_{s}}) + \|WF_{z}\|_{\infty} \gamma_{z}(\bar{\gamma}_{0}, T_{s}) \right),$$
(51)

where

$$\alpha_{3}(T_{s}) \stackrel{\Delta}{=} \max_{t \in [0, MT_{s}]} \|e^{A_{z}t} - \mathbb{I}_{p}\|_{\infty}, \quad \alpha_{4}(T_{s}) \stackrel{\Delta}{=} \max_{t \in [0, MT_{s}]} \int_{0}^{t} \|e^{A_{z}(t-\tau)}\|_{\infty} d\tau.$$
 (52)

Lemma 1. For all $\bar{\gamma}_0 > 0$, the following relationships hold:

$$\lim_{T_s \to 0} \gamma_0(\bar{\gamma}_0, T_s) = 0, \quad \lim_{T_s \to 0} \gamma_r(\bar{\gamma}_0, T_s) = 0, \tag{53}$$

where $\gamma_0(\cdot, \cdot)$ and $\gamma_z(\cdot, \cdot)$ are given in (45) and (51), respectively.

Proof. The proof is similar to the proof of Lemma 3.3.1 in the work of Hovakimyan and Cao^{30} and hence is omitted here.

Lemma 2. There exist $T_s > 0$ and an arbitrarily small positive constant $\bar{\gamma}_0$, such that

$$\gamma_0(\bar{\gamma}_0, T_s) < \bar{\gamma}_0, \quad \Omega_1(T_s)\bar{\gamma}_0 < \bar{\gamma}_1, \quad \gamma_r(\bar{\gamma}_0, T_s) < \bar{\gamma}_r,$$

$$(54)$$

where $\bar{\gamma}_1$ and $\bar{\gamma}_r$ are introduced in (29) and (46). In addition, $\Omega_1(\cdot)$, $\gamma_0(\cdot, \cdot)$, and $\gamma_r(\cdot, \cdot)$ are defined in (39), (45), and (51), respectively.

Proof. It is straightforward to verify that $\Omega_1(T_s)$ is a bounded function as T_s tends to zero. In addition, Lemma 1 shows that $\gamma_0(\bar{\gamma}_0, T_s)$ and $\gamma_z(\bar{\gamma}_0, T_s)$ both approach arbitrarily close to zero for all $\bar{\gamma}_0$ with sufficiently small T_s . Therefore, there always exist constants T_s and $\bar{\gamma}_0$ that satisfy the inequalities in (54).

The sampling time T_s of the digital controller is selected such that $T_s \leq T_{s_{max}}$, and the inequalities in (54) hold.

Lemma 3. For arbitrary $\xi = \begin{bmatrix} y_1 \\ y_2 \end{bmatrix} \in \mathbb{R}^{n_m}$, where $y_1 \in \mathbb{R}^q$ and $y_2 \in \mathbb{R}^{(n_m-q)}$, there exist positive definite $P_1 \in \mathbb{R}^{q \times q}$ and $P_2 \in \mathbb{R}^{(n_m-q) \times (n_m-q)}$ such that

$$\xi^{\mathsf{T}}(\Lambda^{-1})^{\mathsf{T}}P\Lambda^{-1}\xi = y_1^{\mathsf{T}}P_1y_1 + y_2^{\mathsf{T}}P_2y_2,\tag{55}$$

where Λ is given in (19). In addition, P_1 and P_2 are defined in (35).

Proof. The proof of Lemma 3 can be found in the work of Hovakimyan and Cao.³⁰

Consider the following closed-loop reference system:

$$\dot{x}_{\text{ref}}(t) = A_{\text{x}} x_{\text{ref}}(t) + B_{\text{x}} \left(u_{\text{ref}}(t) + f \left(t, x_{\text{ref}}(t) \right) + d(t) \right),
 u_{\text{ref}}(s) = K_{\text{g}} r(s) - C(s) \sigma_{\text{ref}}(s),
 y_{\text{ref}}(t) = C_{\text{x}} x_{\text{ref}}(t), \quad x_{\text{ref}}(0) = x_0,$$
(56)

where

$$\sigma_{\text{ref}}(s) = [(P(s) - P_{\text{m}}(s)) C(s) + P_{\text{m}}(s)]^{-1} (P(s) - P_{\text{m}}(s)) K_{\text{g}} r(s) + [(P(s) - P_{\text{m}}(s)) C(s) + P_{\text{m}}(s)]^{-1} (P(s)w_{\text{ref}}(s) + H_{\text{in}}(s)x_0),$$
(57)

and $w_{ref}(s)$ is the Laplace transform of $w_{ref}(t)$ given by

$$w_{\text{ref}}(t) = F_{x}x_{\text{ref}}(t) + f(t, x_{\text{ref}}(t)) + d(t).$$
 (58)

The reference system can be rewritten as

$$y_{\text{ref}}(s) = P_{\text{m}}(s)K_{\text{g}}r(s) + P_{\text{m}}(s)\left(\mathbb{I}_{q} - C(s)\right)\sigma_{\text{ref}}(s) + C_{\text{m}}\left(s\mathbb{I}_{n_{\text{m}}} - A_{\text{m}}\right)^{-1}C_{\text{m}}^{\dagger}y_{0}.$$
 (59)

From (59), we notice that the unknown uncertainty $\sigma_{ref}(t)$, given by the Laplace transform in (57), is mitigated within the bandwidth of C(s), and the desired response (in Assumption 2) is recovered. The reference system in (56) defines the *achievable performance* by the closed-loop multirate system given in (3), (16)-(22), as the sampling time T_s of the digital controller tends to zero. In the following, we first prove that $\sigma_{ref}(t)$ is bounded, and the reference system in (56) is stable. Then, we establish uniform bounds between the closed-loop system defined by (3), (16)-(22) and the reference system.

Lemma 4. For the closed-loop reference system in (56), subject to the \mathcal{L}_1 -norm condition (33), if $\|x_0\|_{\infty} \leq \rho_0$, then

$$\|x_{\text{ref}}\|_{\mathcal{L}_{\cdot,\cdot}} < \rho_{\text{r}},\tag{60}$$

$$\|u_{\text{ref}}\|_{\mathcal{L}_{\cdot,\cdot}} < \rho_{ur},\tag{61}$$

where ρ_r is introduced in (33), and

$$\rho_{ur} \stackrel{\Delta}{=} \|C(s)H_3(s)\|_{\mathcal{L}_1} \left(L_{\rho_r} \rho_r + L_2 \right) + \|sC(s)H_1(s)P_m^{-1}(s)H_{in}(s)\|_{\mathcal{L}_1} \rho_0 + \left\| \left(\mathbb{I}_q - C(s)H_4(s) \right) K_g \right\|_{\mathcal{L}_1} M_r. \tag{62}$$

Proof. See Appendix A.1 for the proof.

Remark 5. Lemma 4 implies that $\sigma_{ref}(t)$ with Laplace transform defined in (57) is bounded, such that

$$\|\sigma_{\text{ref}}\|_{\mathcal{L}_{\infty}} \le \rho_{\Delta},$$
 (63)

where ρ_{Δ} is defined in (39).

We consider an equivalent state-space model of the predictor dynamics in (17) given by

$$\dot{\hat{x}}(t) = A_{\rm m}\hat{x}(t) + B_{\rm m}u(t) + \hat{\sigma}(t), \quad \hat{x}(0) = C_{\rm m}^{\dagger}y_0
\hat{y}(t) = C_{\rm m}\hat{x}(t),$$
(64)

where

$$\hat{\sigma}(t) = \hat{\sigma}_{d}[j], \quad t \in \left[j \frac{T_{s}}{N}, (j+1) \frac{T_{s}}{N} \right), \quad j \in \mathbb{Z}_{\geq 0}, \tag{65}$$

and u(t) is given by (5) and (16). Since $\hat{\sigma}(t)$ and u(t) are piecewise constants in (64), from (17), we have

$$\hat{y}\left(j\frac{T_{s}}{N}\right) = \hat{y}_{d}[j], \quad j \in \mathbb{Z}_{\geq 0}. \tag{66}$$

Let $\tilde{x}(t) = \hat{x}(t) - x_a(t)$, where $x_a(t)$ is defined in (27). Then, the prediction error dynamics between (27) and (64) are given by

$$\dot{\tilde{x}}(t) = A_{\mathrm{m}}\tilde{x}(t) + \hat{\sigma}(t) - B_{\mathrm{m}}\sigma(t), \quad \tilde{x}(0) = 0_{n_{\mathrm{m}} \times 1},
\tilde{y}(t) = C_{\mathrm{m}}\tilde{x}(t),$$
(67)

where $\hat{\sigma}(t)$ is defined in (65).

Lemma 5. Consider the closed-loop system defined by (3), (16)-(22), and the closed-loop reference system in (56). The following upper bound holds:

$$\|(x_{ref}-x)_t\|_{\mathcal{L}_{\infty}} \leq \Omega_1(T_s)\|\tilde{y}_t\|_{\mathcal{L}_{\infty}},$$

where $\Omega_1(\cdot)$ is given in (39), and $\tilde{y}(t)$ is the prediction error defined in (67).

Proof. See Appendix A.2 for the proof.

Theorem 1. Consider the system in (3) and the controller in (16)-(22) subject to conditions in (32) and (33). Let $\bar{\gamma}_0 > 0$ be a given arbitrarily small constant. Assume that $T_s \leq T_{s_{max}}$ is selected sufficiently small such that the inequalities in (54) hold. If $\|x_0\|_{\infty} \leq \rho_0$, then

$$\|\tilde{y}\|_{\mathcal{L}_{\infty}} < \bar{\gamma}_0, \tag{68}$$

$$||x_{\text{ref}} - x||_{\mathcal{L}_{\infty}} < \Omega_1(T_s)\bar{\gamma}_0, \quad ||u_{\text{ref}} - u||_{\mathcal{L}_{\infty}} < \Omega_2(T_s)\bar{\gamma}_0,$$
 (69)

where $\tilde{y}(t)$ is the prediction error defined in (67). In addition, $\Omega_1(T_s)$ is defined in (39) and

$$\Omega_{2}(T_{s}) \stackrel{\Delta}{=} \|C(s)P_{m}^{-1}(s)\|_{\mathcal{L}_{s}} + \|C(s)\|_{\mathcal{L}_{1}}L_{\rho_{r}}\Omega_{1}(T_{s}) + (N\Gamma(T_{s}) + \Psi(T_{s}))\Upsilon(T_{s}). \tag{70}$$

Proof. See Appendix A.3 for the proof.

Remark 6. Lemmas 1 and 2 indicate that an arbitrarily small bound on the prediction error, $\bar{\gamma}_0$, can be achieved as T_s goes to zero. We can show also that $\Omega_1(T_s)$ and $\Omega_2(T_s)$ are bounded as T_s tends to zero. Therefore, the bounds in (69) can be made arbitrarily small. This implies that the closed-loop SD system recovers the performance of the continuous-time reference system in (56) as the sampling time goes to zero.

Lemma 6. Let $u, v \in \mathbb{R}^q$ with $u = [u_1, \ldots, u_q]^{\top}$ and $v = [v_1, \ldots, v_q]^{\top}$. Suppose that $|v_j| \le 1$ for all $j \in [1, \ldots, q]$. Then, $sat\{u\} \in co\{D_iu + D_i^{\top}v : i \in [1, \ldots, 2^q]\}$, where $co\{\cdot\}$ denotes the convex hull.

Proof. See the work of Hu and Lin⁴⁴ for the proof.

Theorem 2. Consider the high-level subsystem in (4), the desired system in (11), and the reference command law given in (24). Let the positive definite matrix $S \in \mathbb{R}^{p \times p}$ be given. Then, if there exist F_z , $H_z \in \mathbb{R}^{q \times p}$ and a positive definite $R \in \mathbb{R}^{p \times p}$ such that the conditions in (48) and (49) hold, then the error $e_z(t) = z_m(t) - z(t)$ is uniformly bounded such that

$$\|e_{\mathbf{z}}\|_{\mathcal{L}} < \rho_{\mathbf{z}},\tag{71}$$

where ρ_z is given in (50).

Proof. See Appendix A.4 for the proof.

Remark 7. While the error bound ρ_z in (71) remains bounded as the sampling time T_s tends to zero, it cannot be made arbitrarily small. To obtain sufficiently small ρ_z as desired, larger saturation limits (entries of W in (10)) can be chosen, and F_z , F_z , F_z , F_z , and F_z selected accordingly such that (48)-(49) are satisfied.

6 | UAV SIMULATION EXAMPLE

A high-fidelity simulation environment of an UAV is used to verify the effectiveness and advantages of the proposed control framework. To substantiate the existence of a feasible controller that satisfies the theoretical conditions, a multilevel altitude tracking controller is designed for linearized UAV longitudinal dynamics. We then apply the multilevel SD control framework to a high-fidelity UAV simulation platform and compare the multilevel controllers with and without bounded reference signals. At the end, a zero-dynamics attack on altitude measurement is simulated to show the advantages of multirate framework in detecting stealthy attacks.

6.1 | Linearized longitudinal dynamics

A multilevel SD controller is designed for linearized UAV longitudinal dynamics with criteria (33), (48), (49), and (54) fulfilled. Consider the following trim condition within the desired flight operating envelop of an *Ultra Stick*TM25e model UAV⁴⁵: inertial frame position of [0,0,-100] m, body frame velocities of [17,0,0.369] m/s, Euler orientation (roll, pitch, and yaw) of [-0.0983,3.0947,0] deg, surface of elevator at -5.518 deg, aileron and rudder at zero position, throttle at 55.9%, and engine speed at 7897 rpm. Define the state vector $x = (u, w, q, \theta)^{T} \in \mathbb{R}$, where u, w, q, and θ respectively denote the changes of forward velocity, vertical velocity, pitch rate, and pitch angle deviated from the trim condition. With the high-fidelity UAV simulation software developed by the University of Minnesota, 45 the following linearized UAV longitudinal dynamics is considered for the inner-loop dynamics:

$$\dot{x}(t) = A_{x}x(t) + B_{x}\delta_{e}(t), \quad y(t) = \theta(t), \tag{72}$$

where

$$A_{\mathbf{X}} = \begin{pmatrix} -0.5961 & 0.8011 & -0.871 & -9.791 \\ -0.7454 & -7.581 & 15.72 & -0.5272 \\ 1.042 & -7.427 & -15.85 & 0 \\ 0 & 0 & 1 & 0 \end{pmatrix},$$

$$B_{\mathbf{X}} = \begin{pmatrix} 0.4681 - 2.711 - 134.1 & 0 \end{pmatrix}^{\mathsf{T}},$$

$$C_{\mathbf{X}} = \begin{pmatrix} 0 & 0 & 0 & 1 \end{pmatrix},$$

with δ_e , the deviation of elevator surface from the trim condition, being the control input, and the pitch angle θ is chosen as the output for feedback. The outer-loop dynamics from the pitch angle θ to the UAV altitude h takes the form of (73) after linearization

$$\dot{h}(t) = 17 \cdot \theta(t). \tag{73}$$

The models in (72)-(73) represent the nominal linear dynamics. To account for uncertainties in these linear models, we design the controller considering the upper bounds on the additive terms f(t, x(t)) and g(t, x(t)) as defined in (3)-(4). Subject to the dynamical models given in (72) and (73), a multilevel SD controller is designed with the following design parameters: $\rho_0 = 0.01$, $\rho_r = 8.1$, $\alpha = 0.1$, $\bar{\gamma}_1 = 0.015$, $\delta = 0.01$, $\bar{\gamma}_2 = 0.01$, $\mu = 9.4$, M = 1, $\bar{\gamma}_0 = 6.5 \times 10^{-11}$, $G_{\rho_r + \bar{\gamma}_1} = 0.01$, $H_z = 1.177 \times 10^{-3}$, $K_{(\bar{\gamma}_1 + \delta)} = 0.01$, $L_0 = 0.01$, $L_1 = 0.01$,

$$P_{\rm m}(s) = \frac{-1.339 \times 10^{-3} s - 133.9}{s^2 + 134.5s + 1193},\tag{74}$$

and the low-pass filter

$$C(s) = \frac{15\,000}{s + 15\,000}.\tag{75}$$

With the preceding parameters, conditions (33), (48), (49), and (54) are fulfilled, with $\|G(s)\|_{\mathcal{L}_1} = 1.819 \times 10^{-2} < (\rho_r - \rho_1 - \rho_2)/(L_{\rho_r}\rho_r + L_2) = 1.826 \times 10^{-2}$ in (33), $\|WH_z\|_{\infty} = 2.698 \times 10^{-3} < (1-\alpha)\rho_z^{-1} = 2.702 \times 10^{-3}$ in (49), and $\gamma_0(\bar{\gamma}_0, T_s) = 6.369 \times 10^{-11} < \bar{\gamma}_0 = 6.5 \times 10^{-11}$, $\Omega_1(T_s)\bar{\gamma}_0 = 1.468 \times 10^{-2} < \bar{\gamma}_1 = 1.5 \times 10^{-2}$, and $\gamma_r(\bar{\gamma}_0, T_s) = 1.589 \times 10^{-13} < \bar{\gamma}_r = 1.0 \times 10^{-2}$ in (54). In order to satisfy these criteria, the parameters given above are, in some sense, conservative, which can be observed from the following simulation.

With the multilevel SD controller, the UAV to tracks the following reference altitude (height) signal:

$$h_{\rm r}(t) = 10 \cdot \left(\frac{-0.5}{1 + e^{t/5 - 10}} + \frac{1}{1 + e^{t/5 - 40}} - 0.5 \right) + 100. \tag{76}$$

The reference altitude signal $h_r(t)$ and the UAV altitude h(t) are given in Figure 2. Due to the conservativeness of design parameters, certain amount of tracking error exists in Figure 2, which can be efficiently reduced by increasing the proportional gain F_z in outer-loop controller. Figure 3 shows the commanded pitch angle $h_r(t)$ generated by the outer-loop controller, UAV pitch angle $\theta(t)$, and the deviation of the elevator surface $\delta_e(t)$. From the result, one can see that the reference signal r(t) is within the bound $M_r = 0.4363$ rad $\approx 25^\circ$; the UAV pitch angle $\theta(t)$ tracks the reference pitch angle r(t) precisely with the multirate \mathcal{L}_1 inner-loop controller, and the deviation of the elevator is also within the saturation bound.

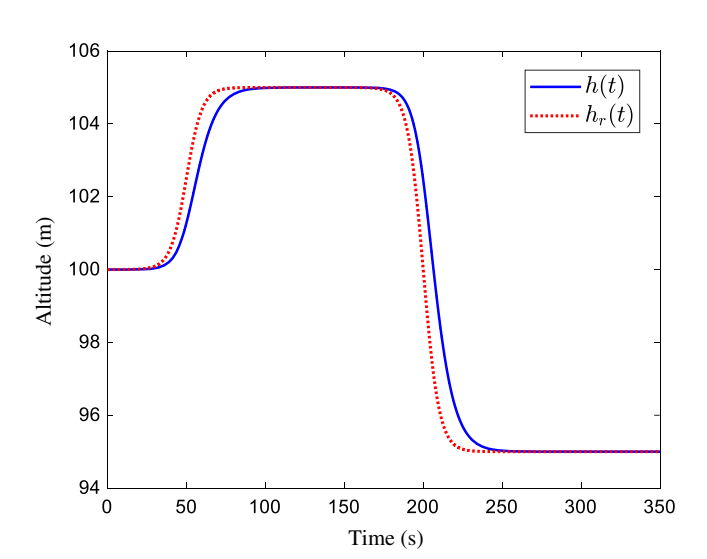


FIGURE 2 The unmanned aerial vehicle tracks the desired altitude [Colour figure can be viewed at wileyonlinelibrary.com]

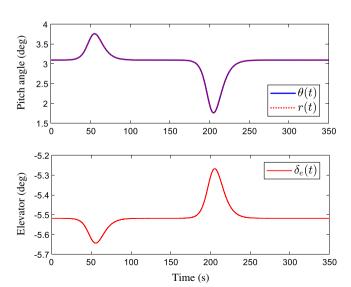


FIGURE 3 Pitch angle $\theta(t)$ and elevator deviation δ_e [Colour figure can be viewed at wileyonlinelibrary.com]

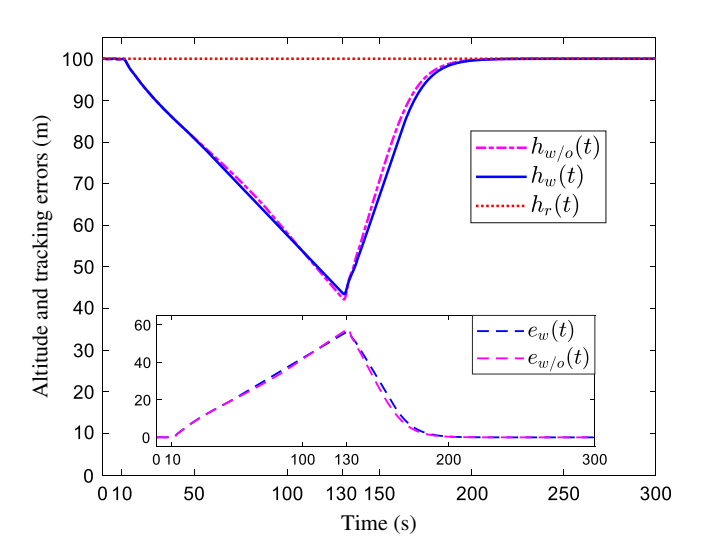


FIGURE 4 Altitudes and tracking errors under the motor failure scenario [Colour figure can be viewed at wileyonlinelibrary.com]

6.2 | Nonlinear model with motor failures

After we showed the existence of a feasible controller with the linearized UAV longitudinal dynamics, we then test this multilevel SD control framework in a high-fidelity UAV simulation environment.⁴⁵ Assume that the lateral dynamics is stabilized by some existing controller along the roll and yaw channels and consider a scenario when the propulsion level of UAV decreases by 80% for two minutes (as a large unplanned uncertainty), while the UAV still tries to track a commanded altitude signal at $h_r(t) = 100$. The saturation limits of UAV elevator are $\pm 25^{\circ}$. Some design parameters are adjusted to adapt to the high-fidelity UAV dynamics and environmental factors. The desired dynamics is selected as

$$P_{\rm m}(s) = \frac{-0.2067s - 20.67}{s^2 + 2.9s + 3.793},\tag{77}$$

with the low-pass filter

$$C(s) = \frac{4}{s+4}. (78)$$

The sampling period is $T_s = 0.02$, and all the other parameters are unaltered. We compare a multilevel controller with reference pitch angle $r_w(t)$ constrained by saturation bounds within $[-11^\circ, 11^\circ]$ and a multilevel controller with unconstrained reference signal $r_{w/o}(t)$. This constraint does not limit the maneuverability of the UAV since the safety constraint is on the generated command signal, not on the actuators.

In the following simulation, we use subscript "w" to denote the results of control scheme with bounded reference signal, while subscript "w/o" is used to denote the results of control scheme with unconstrained reference signal. The reference altitude signal $h_r(t)$, UAV altitudes $h_w(t)$ and $h_{w/o}(t)$, and the tracking errors $e_w(t)$ and $e_{w/o}(t)$ are shown in Figure 4. The reference pitch angles $r_w(t)$ and $r_{w/o}(t)$, UAV pitch angles $\theta_w(t)$ and $\theta_{w/o}(t)$, angles of attack $\alpha_w(t)$ and $\alpha_{w/o}(t)$, and the deviations of elevator $\delta_{e,w}(t)$ and $\delta_{e,w/o}(t)$ are given in Figure 5. It can be observed that although the reference pitch angle is confined inside an envelope, the difference between altitudes $h_w(t)$ and $h_{w/o}(t)$ is small. Meanwhile, the bounded reference pitch angle $r_w(t)$ prevents the elevator from saturation and keeps the pitch angle $\theta_w(t)$ and the angle of attack $\alpha_w(t)$ inside a relatively safer envelope, in which the UAV is less likely to crash or stall. It is clear that the multilevel SD control framework with bounded reference signal ensures safety of the autonomous UAV in the presence of uncertainties.

6.3 | Full-state dynamics under zero-dynamics attacks

The multirate control scheme is also able to detect the stealthy zero-dynamics attacks. In this last example, we show a zero-dynamics attack on a full-state UAV trim model via GPS or altimeter spoofing. With the same trim condition, when the sampling period of digital control system is $T_s = 5T = 0.1$ seconds, while the faster output sampling period is T = 0.02 seconds, discretizing the continuous transfer function from the elevator δ_e to the UAV altitude h(t) with the sampling period T_s generates a nonminimum-phase zero at z = -6.0108, which can be used for stealthy attack. The attack signal is generated by adding the following zero-dynamics attack signal

$$h_{a}(t) = h_{a,i}[i], \quad t \in [iT_s, (i+1)T_s), \quad h_{a,i}[i] = \epsilon(-6.0108)^{iT_s}, \quad i \in \mathbb{Z}_{\geq 0}$$
 (79)

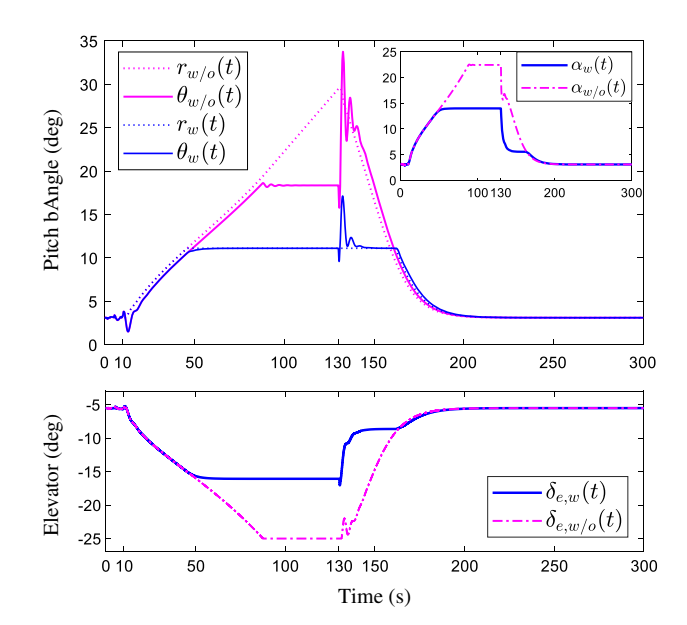


FIGURE 5 Pitch angles and elevator deviations under the motor failure scenario [Colour figure can be viewed at wileyonlinelibrary.com]

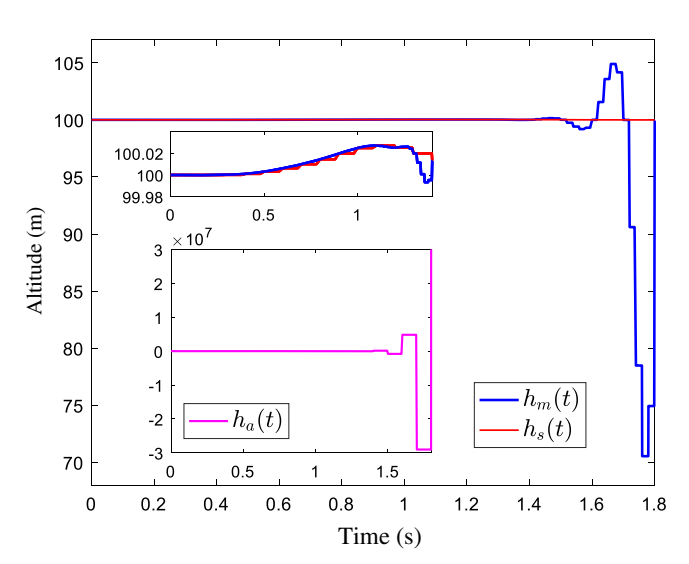


FIGURE 6 Pitch angle θ with the linearized unmanned aerial vehicle model under the zero-dynamics attack [Colour figure can be viewed at wileyonlinelibrary.com]

into the normal altitude measurement signal h(t), where $\epsilon=10^{-5}$. Under the zero-dynamics attack and in the presence of measurement noise, Figure 6 shows the zero-dynamics attack signal $h_a(t)$, altitude measurements from a single-rate controller $h_s(t)$, and the altitude measurement from a multirate adaptive controller $h_m(t)$. It is apparent that the single rate controller is not able to detect the drastic changes of UAV height caused by the zero-dynamics attack, while the multirate \mathcal{L}_1 controller can detect this anomaly at a relative earlier stage despite the contamination of measurement noise.

Remark 8. After detection, zero-dynamics attack can be removed by considering a secure software/hardware architecture (simplex design^{46,47}). In such structure, a backup controller will operate the system, when the normal mode controller is compromised due to a cyber attack. By switching from the normal mode to a secured backup controller, the unbounded stealthy attack can be removed (from the cyber space). Then, the backup controller can recover the stability of the perturbed system. For successful recovery, early detection is critical. Reader can see the works of Jafarnejadsani et al^{42,48} for more details.

Remark 9. As shown in the numerical example of Section 6.1, while the sufficient theoretical stability conditions are conservative, one can find a set of design parameters that satisfy all of the theoretical conditions (feasibility). As demonstrated in the nonlinear high-fidelity UAV example of Section 6.2, the proposed control structure effectively allows for design of the control parameters to practically balance the trade-offs between performance and robustness, without the requirement to satisfy the sufficient stability conditions. On the other hand, the assumptions made in this paper are not conservative. We consider a class of uncertain MIMO systems subject to nested saturation, where



only some of the states are available for measurement. A less-restrictive assumption of locally Lipschitz continuity is employed for unknown nonlinear terms, and the dynamics of the system can be nonminimum-phase. This paper introduces a challenging problem in output-feedback control for SD systems which has only been dealt with in very few study.

7 | CONCLUSION

For safe and secure control of autonomous systems in the presence of uncertainties, physical failures, and cyber attacks, a multilevel SD control structure is proposed. For this purpose, a class of nested uncertain MIMO systems subject to reference command saturation, possibly with nonminimum phase zeros, is considered. The multirate SD approach of this paper facilitates the implementation of controller on digital computers, where the input/output signals are available at discrete-time instances with different sampling rates. In addition, the stealthy zero-dynamics attacks become detectable by considering a multirate formulation.

ACKNOWLEDGEMENTS

This work has been supported in part by National Science Foundation and Air Force Office of Scientific Research (AFOSR).

ORCID

Hamidreza Jafarnejadsani https://orcid.org/0000-0002-8489-005X

REFERENCES

- 1. Mohan N, Undeland TM. Power Electronics: Converters, Applications, and Design. Hoboken, NJ: John Wiley & Sons; 2007.
- 2. Zarchan P. Tactical and Strategic Missile Guidance. Reston, VA: American Institute of Aeronautics and Astronautics, Inc.; 2012.
- 3. Shtessel Y, Buffington J, Banda S. Tailless aircraft flight control using multiple time scale reconfigurable sliding modes. *IEEE Trans Control Syst Technol.* 2002;10(2):288-296.
- 4. Voos H. Nonlinear control of a quadrotor micro-UAV using feedback-linearization. Paper presented at: IEEE International Conference on Mechatronics; 2009; Malaga, Spain.
- 5. Cao N, Lynch AF. Inner-outer loop control for quadrotor UAVs with input and state constraints. *IEEE Trans Control Syst Technol*. 2016;24(5):1797-1804.
- 6. Kendoul F, Fantoni I, Lozano R, et al. Asymptotic stability of hierarchical inner-outer loop-based flight controllers. In: Proceedings of the 17th IFAC World Congress; 2008; Seoul, South Korea.
- 7. Nicotra MM, Garone E, Naldi R, Marconi L. Nested saturation control of an UAV carrying a suspended load. Paper presented at: American Control Conference (ACC); 2014; Portland, OR.
- 8. Castillo P, Lozano R, Dzul A. Stabilization of a mini rotorcraft with four rotors. IEEE Control Syst Mag. 2005;25(6):45-55.
- 9. Metni N, Hamel T. A UAV for bridge inspection: visual servoing control law with orientation limits. Autom Constr. 2007;17(1):3-10.
- 10. Teel AR. Global stabilization and restricted tracking for multiple integrators with bounded controls. Syst Control Lett. 1992;18(3):165-171.
- 11. Chen T, Francis BA. Optimal Sampled-Data Control Systems. New York, NY: Springer Science & Business Media; 2012.
- 12. Nesic D, Teel AR, Carnevale D. Explicit computation of the sampling period in emulation of controllers for nonlinear sampled-data systems. *IEEE Trans Autom Control*. 2009;54(3):619-624.
- 13. Lin W, Wei W. Robust stabilization of nonminimum-phase systems with uncertainty by sampled-data output feedback. Paper presented at: 55th IEEE Conference on Decision and Control; 2016; Las Vegas, NV.
- 14. Chu H, Qian C, Yang J, Xu S, Liu Y. Almost disturbance decoupling for a class of nonlinear systems via sampled-data output feedback control. *Int J Robust Nonlinear Control*. 2015;26(10):2201-2215.
- 15. Khalil HK. Performance recovery under output feedback sampled-data stabilization of a class of nonlinear systems. *IEEE Trans Autom Control*. 2004;49(12):2173-2184.
- 16. Ahrens JH, Tan X, Khalil HK. Multirate sampled-data output feedback control with application to smart material actuated systems. *IEEE Trans Autom Control*. 2009;54(11):2518-2529.
- 17. Ahmed Ali S, Langlois N, Guermouche M. Sampled-data disturbance observer for a class of nonlinear systems. Paper presented at: 19th IFAC World Congress; 2014; Cape Town, South Africa.
- 18. Shim H, Teel AR. Asymptotic controllability and observability imply semiglobal practical asymptotic stabilizability by sampled-data output feedback. *Automatica*. 2003;39(3):441-454.
- 19. Lam HK. Stabilization of nonlinear systems using sampled-data output-feedback fuzzy controller based on polynomial-fuzzy-model-based control approach. *IEEE Trans Syst Man Cybern Part B (Cybern)*. 2012;42(1):258-267.

- 20. Qian C, Du H. Global output feedback stabilization of a class of nonlinear systems via linear sampled-data control. *IEEE Trans Autom Control*. 2012;57(11):2934-2939.
- 21. Zhang C, Yang J. Semi-global sampled-data output feedback disturbance rejection control for a class of uncertain nonlinear systems. *Int J Syst Sci.* 2016;48(4)::757-768.
- 22. Liu W, Ma Q, Jia X. Sampled-data output feedback control for a class of nonlinear systems with mismatched disturbances. Paper presented at: 35th Chinese Control Conference (CCC); 2016; Chengdu, China.
- 23. Lin W, Wei W. Robust control of a family of uncertain nonminimum-phase systems via continuous-time and sampled-data output feedback. *Int J Robust Nonlinear Control*. 2017;28(4):1440-1455.
- 24. Guillaume A-M, Bastin G, Campion G. Sampled-data adaptive control of a class of continuous nonlinear systems. *Int J Control*. 1994;60(4):569-594.
- 25. Wu B, Ding Z. A sampled-data scheme for adaptive control of nonlinear systems. Paper presented at: American Control Conference; 2007; New York, NY.
- 26. Laila DS, Navarro-López EM, Astolfi A. Sampled-data adaptive control for a class of nonlinear systems with parametric uncertainties. *IFAC Proc Vol.* 2011;44(1):1261-1266.
- 27. Chen T, Francis B. Optimal Sampled-Data Control Systems. London, UK: Springer; 1995.
- 28. Naghnaeian M, Hirzallah N, Voulgaris PG. Dual rate control for security in cyber-physical systems. Paper presented at: 54th IEEE Conference on Decision and Control; 2015; Osaka, Japan.
- 29. Cao C, Hovakimyan N. Design and analysis of a novel \mathcal{L}_1 adaptive control architecture with guaranteed transient performance. *IEEE Trans Autom Control*. 2008;53(2):586-591.
- 30. Hovakimyan N, Cao C. \mathcal{L}_1 Adaptive Control Theory: Guaranteed Robustness With Fast Adaptation. Philadelphia, PA: Society for Industrial and Applied Mathematics; 2010.
- 31. Cao C, Hovakimyan N. \mathcal{L}_1 adaptive output-feedback controller for nonstrictly-positive-real reference systems: missile longitudinal autopilot design. *J Guid Control Dyn.* 2009;32(3):717-726.
- 32. Ackerman K, Xargay E, Choe R, et al. L1 stability augmentation system for Calspan's variable-stability Learjet. Paper presented at: AIAA Guidance, Navigation, and Control Conference; 2016; San Diego, CA.
- 33. Cotting MC, Jeffrey RB, Blackstun MP, et al. 'Can I get L1 on?!' Providing consistent handling qualities on Calspan's variable-stability Learjet. Paper presented at: AIAA Guidance, Navigation, and Control Conference; 2016; San Diego, CA.
- 34. Gregory I, Xargay E, Cao C, Hovakimyan N. Flight test of an L1 adaptive controller on the NASA AirSTAR flight test vehicle. Paper presented at: AIAA Guidance, Navigation, and Control Conference; 2010; Toronto, Canada.
- 35. Lee H, Snyder S, Hovakimyan N. An adaptive unknown input observer for fault detection and isolation of aircraft actuator faults. Paper presented at: AIAA Guidance, Navigation, and Control Conference; 2014.
- 36. Lee H, Snyder S, Hovakimyan N. L1 adaptive control within a flight envelope protection system. J Guid Control Dyn. 2017;40(4):1013-1026.
- 37. Cao C, Hovakimyan N, Patel VV, Kaminer I, Dobrokhodov V. Stabilization of cascaded systems via L1 adaptive controller with application to a UAV path following problem and flight test results. Paper presented at: American Control Conference; 2007; New York, NY.
- 38. Jafarnejadsani H, Sun D, Lee H, Hovakimyan N. Optimized L1 adaptive controller for trajectory tracking of an indoor quadrotor. *J Guid Control Dyn.* 2017;40(6):1415-1427.
- 39. Leman T, Xargay E, Dullerud G, Hovakimyan N, Wendel T. L1 adaptive control augmentation system for the x-48B aircraft. Paper presented at: AIAA Guidance, Navigation, and Control Conference; 2009; Chicago, IL.
- 40. Cao C, Hovakimyan N. Stability margins of L₁ adaptive control architecture. *IEEE Trans Autom Control*. 2010;55:480-487.
- 41. Jafarnejadsani H, Lee H, Hovakimyan N, Voulgaris PG. Dual-rate L1 adaptive controller for cyber-physical sampled-data systems. Paper presented at: IEEE 56th Annual Conference on Decision and Control (CDC); 2017; Melbourne, Australia.
- 42. Jafarnejadsani H, Lee H, Hovakimyan N, Voulgaris P. A multirate adaptive control for MIMO systems with application to cyber-physical security. Paper presented at: IEEE 57th Conference on Decision and Control (CDC); 2018; Miami Beach, FL.
- 43. Fang H, Lin Z, Hu T. Analysis of linear systems in the presence of actuator saturation and L2-disturbances. *Automatica*. 2004;40(7):1229-1238.
- 44. Hu T, Lin Z. Control Systems With Actuator Saturation: Analysis and Design. New York, NY: Springer Science & Business Media; 2001.
- 45. Paw YC. Synthesis and Validation of Flight Control for UAV [PhD thesis]. Minneapolis, MN: University of Minnesota; 2009.
- 46. Sha L. Using simplicity to control complexity. IEEE Software. 2001;18(4):20-28.
- 47. Wang X, Hovakimyan N, Sha L. L1simplex: fault-tolerant control of cyber-physical systems. In: Proceedings of the ACM/IEEE 4th International Conference on Cyber-Physical Systems ACM; 2013; Philadelphia, PA.
- 48. Jafarnejadsani H, Lee H, Hovakimyan N. An \mathcal{L}_1 adaptive control design for output-feedback sampled-data systems. Paper presented at: American Control Conference; 2017; Seattle, WA.

How to cite this article: Jafarnejadsani H, Wan N, Hovakimyan N, Voulgaris PG. A multilevel sampled-data approach for resilient navigation and control of autonomous systems. *Int J Robust Nonlinear Control*. 2020;30:1071–1097. https://doi.org/10.1002/rnc.4814

APPENDIX A

A.1 | Proof of Lemma 4

It follows from (56) and the definition of $H_0(s)$, $H_5(s)$, P(s), and G(s) in (26) that

$$x_{\text{ref}}(s) = [H_0(s) - H_5(s)(P(s) - P_m(s))]K_gr(s) - G(s)w_{\text{ref}}(s) - H_5(s)H_{\text{in}}(s)x_0 + (s\mathbb{I}_n - A_x + B_xF_x)^{-1}x_0.$$

Then, the following upper bound can be established for $\tau > 0$

$$\|x_{\text{ref}_{\tau}}\|_{\mathcal{L}_{\infty}} \leq \|G(s)\|_{\mathcal{L}_{1}} \|w_{\text{ref}_{\tau}}\|_{\mathcal{L}_{\infty}} + \|H_{2}(s)K_{g}\|_{\mathcal{L}_{1}} \|r\|_{\mathcal{L}_{\infty}} + \left\|s(s\mathbb{I}_{n} - A_{x} + B_{x}F_{x})^{-1} - sH_{5}(s)H_{\text{in}}(s)\right\|_{\mathcal{L}_{1}} \left\|\frac{1}{s}x_{0}\right\|_{\mathcal{L}_{\infty}}. \tag{A1}$$

We have $||x_{\text{ref}}(0)||_{\infty} = ||x_0||_{\infty} < \rho_r$. In addition, $x_{\text{ref}}(t)$ is continuous. Therefore, if the bound in (60) is not true, there exists a time $\tau_1 > 0$ such that

$$||x_{\text{ref}}(t)||_{\infty} < \rho_{\text{r}}, \quad \forall t \in [0, \tau_1), \quad ||x_{\text{ref}}(\tau_1)||_{\infty} = \rho_{\text{r}},$$

which implies that $||x_{\text{ref}\tau_1}||_{\mathcal{L}_{\infty}} = \rho_r$. Then, it follows from Assumption 1 and the redefinition in (29) that

$$\|w_{\text{ref}_{\tau_1}}\|_{\mathcal{L}_{\infty}} \le L_{\rho_r} \|x_{\text{ref}_{\tau_1}}\|_{\mathcal{L}_{\infty}} + L_2.$$
 (A2)

The bound in (A2), together with the upper bound in (A1), leads to

$$\|x_{\operatorname{ref}_{\tau_1}}\|_{\mathcal{L}_{\infty}} \le \frac{\|G(s)\|_{\mathcal{L}_1} L_2 + \rho_1 + \rho_2}{1 - \|G(s)\|_{\mathcal{L}_1} L_{\rho_s}}.$$

The condition in (33) can be solved for ρ_r to obtain the bound

$$\rho_{\rm r} > \frac{\|G(s)\|_{\mathcal{L}_1} L_2 + \rho_1 + \rho_2}{1 - \|G(s)\|_{\mathcal{L}_s} L_a},$$

which leads to $\|x_{\text{ref}\tau_1}\|_{\mathcal{L}_{\infty}} < \rho_r$. This contradicts $\|x_{\text{ref}\tau_1}\|_{\mathcal{L}_{\infty}} = \rho_r$, thus proving the bound in (60). This further implies that the upper bound in (A2) holds for all $\tau_1 > 0$ with strict inequality, which in turn implies that

$$\|w_{\text{ref}}\|_{\mathcal{L}_{u}} < L_{\rho_{x}}\rho_{r} + L_{2}.$$
 (A3)

The bound on $u_{ref}(t)$ follows from (56), (57), and (A3), which proves (61).

A.2 | Proof of Lemma 5

Let

$$u_{C}(s) = K_{g}r(s) - C(s)P_{m}^{-1}(s)C_{m}(s\mathbb{I}_{n_{m}} - A_{m})^{-1}\hat{\sigma}(s), \tag{A4}$$

$$u_{\rm M}(s) = K_{\rm g} r(s) - C(s) P_{\rm m}^{-1}(s) C_{\rm m} \left(s \mathbb{I}_{n_{\rm m}} - A_{\rm m}\right)^{-1} e^{-A_{\rm m} \frac{T_{\rm s}}{N}} \hat{\sigma}(s). \tag{A5}$$

It follows from (67) that

$$\tilde{y}(s) = -P_{\mathbf{m}}(s)\sigma(s) + C_{\mathbf{m}}(s\mathbb{I}_{n_{\mathbf{m}}} - A_{\mathbf{m}})^{-1}\hat{\sigma}(s). \tag{A6}$$

Letting $e(t) \stackrel{\Delta}{=} x_{\text{ref}}(t) - x(t)$ and denoting by $d_{e}(s)$ the Laplace transform of

$$d_{e}(t) \stackrel{\Delta}{=} w_{ref}(t) - w(t), \tag{A7}$$

from (3), (28), (16), (56), (A4), (A5), and (A6), it follows

$$e(s) = H_0(s)C(s)P_m^{-1}(s)\tilde{y}(s) + H_0(s)d_e(s) + H_0(s)(u_C(s) - u_M(s)) + H_0(s)(u_M(s) - u(s)) - H_0(s)C(s)(\sigma_{ref}(s) - \sigma(s)),$$
 (A8)

where $H_0(s)$ is defined in (26). Furthermore,

$$H_{0}(s)C(s) \left(\sigma_{\text{ref}}(s) - \sigma(s)\right) = H_{5}(s)P(s)d_{e}(s) - H_{5}(s) \left(P(s) - P_{\text{m}}(s)\right) \left(u_{\text{C}}(s) - u_{\text{M}}(s)\right) - H_{5}(s) \left(P(s) - P_{\text{m}}(s)\right) \left(u_{\text{M}}(s) - u(s)\right) + H_{5}(s) \left(P(s) - P_{\text{m}}(s)\right) C(s)P_{\text{m}}^{-1}(s)\tilde{y}(s).$$
(A9)

From (A8) and (A9), one can obtain

$$\begin{split} e(s) &= \left(H_0(s) - H_5(s)\left(P(s) - P_{\rm m}(s)\right)\right)C(s)P_{\rm m}^{-1}(s)\tilde{y}(s) + \left(H_0(s) - H_5(s)\left(P(s) - P_{\rm m}(s)\right)\right)\left(u_{\rm C}(s) - u_{\rm M}(s)\right) \\ &+ \left(H_0(s) - H_5(s)\left(P(s) - P_{\rm m}(s)\right)\right)\left(u_{\rm M}(s) - u(s)\right) + \left(H_0(s) - H_5(s)P(s)\right)d_{\rm e}(s). \end{split} \tag{A10}$$

Then, the upper bound is given by

$$\begin{aligned} \|e_{t}\|_{\mathcal{L}_{\infty}} &\leq \|(H_{0}(s) - H_{5}(s) (P(s) - P_{m}(s))) C(s) P_{m}^{-1}(s) \|_{\mathcal{L}_{1}} \|\tilde{y}_{t}\|_{\mathcal{L}_{\infty}} + \|(H_{0}(s) - H_{5}(s) (P(s) - P_{m}(s))) \|_{\mathcal{L}_{1}} \|(u_{C} - u_{M})_{t} \|_{\mathcal{L}_{\infty}} \\ &+ \|(H_{0}(s) - H_{5}(s) (P(s) - P_{m}(s))) \|_{\mathcal{L}_{1}} \|(u_{M} - u)_{t} \|_{\mathcal{L}_{\infty}} + \|G(s) \|_{\mathcal{L}_{1}} L_{\rho_{r}} \|e_{t} \|_{\mathcal{L}_{\infty}}. \end{aligned}$$

$$(A11)$$

From (66), we have

$$\tilde{y}\left(j\frac{T_{\rm s}}{N}\right) = \tilde{y}_{\rm d}[j], \quad j \in \mathbb{Z}_{\geq 0}.$$
 (A12)

From (22), (65), and (A12), the following relation holds:

$$\left\| e^{-A_{\mathrm{m}} \frac{T_{\mathrm{s}}}{N}} \hat{\sigma}_{t} \right\|_{\mathcal{L}_{\infty}} \leq \Upsilon \left(T_{\mathrm{s}} \right) \left\| \tilde{y}_{t} \right\|_{\mathcal{L}_{\infty}}, \tag{A13}$$

where $\Upsilon(\cdot)$ is defined in (39). Notice that $u_d[i]$ given in (16) is a step-invariant discrete-time approximation of $u_M(s)$, given in (A5). Therefore, the discretization error bound between (5) and (A5) is given by

$$\|(u_{\mathcal{M}} - u)_t\|_{\mathcal{L}_{\infty}} \le N\Gamma(T_{\mathcal{S}}) \Upsilon(T_{\mathcal{S}}) \|\tilde{y}_t\|_{\mathcal{L}_{\infty}},\tag{A14}$$

where $\Gamma(\cdot)$ is introduced in (38). Moreover, from (A4), (A5), and (A13), one can obtain

$$\|(u_{\mathcal{C}} - u_{\mathcal{M}})_t\|_{\mathcal{L}} \le \Psi(T_{\mathcal{S}}) \Upsilon(T_{\mathcal{S}}) \|\tilde{y}_t\|_{\mathcal{L}_{\mathcal{L}}},$$
 (A15)

where $\Psi(\cdot)$ is defined in (39). From (A11), (A14), and (A15), the following upper bound holds:

$$\|e_t\|_{\mathcal{L}_{\ldots}} \le \Omega_1(T_s) \|\tilde{y}_t\|_{\mathcal{L}_{\ldots}}. \tag{A16}$$

This concludes the proof.

A.3 | Proof of Theorem 1

Let $\bar{\gamma}_0$ be a constant satisfying (54). First, we prove the bound in (68) by a contradiction argument. Since $\tilde{y}(0) = 0$, and $\tilde{y}(t)$ is continuous, then assuming the opposite implies that there exists τ_1 such that

$$\|\tilde{y}(t)\|_{\infty} < \bar{\gamma}_0, \quad \forall 0 \le t < \tau_1,$$

$$\|\tilde{y}(\tau_1)\|_{\infty} = \bar{\gamma}_0,$$
(A17)

which leads to

$$\left\|\tilde{y}_{\tau_1}\right\|_{\mathcal{L}_{\infty}} = \bar{\gamma}_0. \tag{A18}$$

Let $e(t) = x_{ref}(t) - x(t)$. The sampling time T_s is selected such that the inequities in (54) hold. Then, the bound in (54), Lemma 5, and the upper bound in (60) can be used to derive the following bound

$$\|x_{\tau_1}\|_{\mathcal{L}_{\infty}} \le \|x_{\text{ref}_{\tau_1}}\|_{\mathcal{L}_{\infty}} + \|e_{\tau_1}\|_{\mathcal{L}_{\infty}} < \rho_{\text{r}} + \bar{\gamma}_1, \tag{A19}$$

which implies

$$\|w_{\tau_1}\|_{\mathcal{L}_{\infty}} \le L_{\rho_r} \rho_r + L_2.$$
 (A20)

One can obtain from (57) that

$$\left\|\sigma_{\operatorname{ref}_{r_1}}\right\|_{\mathcal{L}_{\infty}} \le \rho_{\Delta},\tag{A21}$$

where ρ_{Δ} is defined in (39). In addition, we have

$$\sigma_{\text{ref}}(s) - \sigma(s) = H_3(s)d_e(s) - H_4(s)\left(u_{\text{M}}(s) - u(s)\right) - H_4(s)\left(u_{\text{C}}(s) - u_{\text{M}}(s)\right) + H_4(s)C(s)P_{\text{m}}^{-1}(s)\tilde{y}(s), \tag{A22}$$

which along with (A21) implies

$$\|\sigma_{\tau_{i}}\|_{\mathcal{L}_{i,i}} \le \Delta_{1}(\bar{\gamma}_{0}),\tag{A23}$$

where $\Delta(\cdot)$ is defined in (43).

Now, consider the state transformation

$$\tilde{\xi} = \Lambda \tilde{x},\tag{A24}$$

where Λ is defined in (19), and $\tilde{x}(t) = \hat{x}(t) - x_a(t)$. From (67) and (A24), it follows

$$\dot{\tilde{\xi}}(t) = \Lambda A_{\mathrm{m}} \Lambda^{-1} \tilde{\xi}(t) + \Lambda \hat{\sigma}(t) - \Lambda B_{\mathrm{m}} \sigma(t),
\tilde{y}(t) = \mathbf{1}_{n_{\mathrm{m}} q} \tilde{\xi}(t), \quad \tilde{\xi}(0) = 0_{n_{\mathrm{m}} \times 1}.$$
(A25)

From (A25), we have

$$\tilde{\xi}\left(j\frac{T_{\rm s}}{N}+t\right) = e^{\Lambda A_{\rm m}\Lambda^{-1}t}\tilde{\xi}\left(j\frac{T_{\rm s}}{N}\right) + \int_0^t e^{\Lambda A_{\rm m}\Lambda^{-1}(t-\tau)}\Lambda\left(\hat{\sigma}\left(j\frac{T_{\rm s}}{N}\right) - B_{\rm m}\sigma\left(j\frac{T_{\rm s}}{N}+\tau\right)\right)d\tau. \tag{A26}$$

Since

$$\tilde{\xi}\left(j\frac{T_{\rm s}}{N}+t\right) = \begin{bmatrix} \tilde{y}\left(j\frac{T_{\rm s}}{N}+t\right) \\ 0_{(n_{\rm m}-q)\times 1} \end{bmatrix} + \begin{bmatrix} 0_{q\times 1} \\ \tilde{z}\left(j\frac{T_{\rm s}}{N}+t\right) \end{bmatrix},$$

where $\tilde{z}(t) = \left[\tilde{\xi}_{q+1}(t), \ldots, \tilde{\xi}_{n_{\rm m}}(t)\right]^{\mathsf{T}}, \tilde{\xi}(j\frac{T_{\rm s}}{N} + t)$ can be decomposed as

$$\tilde{\xi}\left(j\frac{T_{\rm s}}{N}+t\right) = \chi\left(j\frac{T_{\rm s}}{N}+t\right) + \zeta\left(j\frac{T_{\rm s}}{N}+t\right),\tag{A27}$$

such that

$$\chi\left(j\frac{T_{\rm s}}{N}+t\right) = e^{\Lambda A_{\rm m}\Lambda^{-1}t} \begin{bmatrix} \tilde{y}\left(j\frac{T_{\rm s}}{N}\right) \\ 0_{(n_{\rm m}-q)\times 1} \end{bmatrix} + \int_0^t e^{\Lambda A_{\rm m}\Lambda^{-1}(t-\tau)}\Lambda\hat{\sigma}\left(j\frac{T_{\rm s}}{N}\right)d\tau, \tag{A28}$$

$$\zeta\left(j\frac{T_{\rm s}}{N}+t\right) = e^{\Lambda A_{\rm m}\Lambda^{-1}t} \begin{bmatrix} 0_{q\times 1} \\ \tilde{z}\left(j\frac{T_{\rm s}}{N}\right) \end{bmatrix} - \int_0^t e^{\Lambda A_{\rm m}\Lambda^{-1}(t-\tau)} \Lambda B_{\rm m}\sigma\left(j\frac{T_{\rm s}}{N}+\tau\right) d\tau. \tag{A29}$$

Next, we prove that

$$\left\| \tilde{y} \left(j \frac{T_{s}}{N} \right) \right\|_{2} \leq \varsigma(\tilde{y}_{0}, T_{s}), \quad \tilde{z}^{\mathsf{T}} \left(j \frac{T_{s}}{N} \right) P_{2} \tilde{z} \left(j \frac{T_{s}}{N} \right) \leq \Delta_{2}(\tilde{y}_{0}), \quad \forall j \frac{T_{s}}{N} \leq \tau_{1}, \tag{A30}$$

where $\Delta(\cdot)$ and $\varsigma(\cdot, \cdot)$ are defined in (43) and (44), respectively. It is straightforward to show that $\|\tilde{y}(0)\|_2 \leq \varsigma(\bar{\gamma}_0, T_s)$, $\tilde{z}^{\mathsf{T}}(0)P_2\tilde{z}(0) \leq \Delta_2(\bar{\gamma}_0)$. Next, for arbitrary $k \in \mathbb{Z}_{\geq 0}$ such that $(k+1)\frac{T_s}{N} \leq \tau_1$, we prove that if

$$\left\| \tilde{y} \left(k \frac{T_{s}}{N} \right) \right\|_{2} \le \zeta(\bar{\gamma}_{0}, T_{s}), \tag{A31}$$

$$\tilde{z}^{\mathsf{T}}\left(k\frac{T_{\mathsf{s}}}{N}\right)P_{2}\tilde{z}\left(k\frac{T_{\mathsf{s}}}{N}\right) \leq \Delta_{2}(\bar{\gamma}_{0}),$$
(A32)

then the inequalities in (A31)-(A32) hold for k+1 as well, which would imply that the bounds in (A31)-(A32) hold for all $k \in \mathbb{Z}_{\geq 0}$ such that $k \frac{T_s}{N} \leq \tau_1$. To this end, suppose that (A31) and (A32) hold for $k \in \mathbb{Z}_{\geq 0}$, and in addition that $(k+1) \frac{T_s}{N} \leq \tau_1$. Then, it follows from (A27) that

$$\tilde{\xi}\left((k+1)\frac{T_{\rm s}}{N}\right) = \chi\left((k+1)\frac{T_{\rm s}}{N}\right) + \zeta\left((k+1)\frac{T_{\rm s}}{N}\right),\tag{A33}$$

where

$$\chi\left((k+1)\frac{T_{s}}{N}\right) = e^{\Lambda A_{m}\Lambda^{-1}\frac{T_{s}}{N}} \begin{bmatrix} \tilde{y}\left(k\frac{T_{s}}{N}\right) \\ 0_{(n_{m}-q)\times 1} \end{bmatrix} + \int_{0}^{\frac{T_{s}}{N}} e^{\Lambda A_{m}\Lambda^{-1}\left(\frac{T_{s}}{N}-\tau\right)} \Lambda \hat{\sigma}\left(k\frac{T_{s}}{N}\right) d\tau,$$

$$\zeta\left((k+1)\frac{T_{s}}{N}\right) = e^{\Lambda A_{m}\Lambda^{-1}\frac{T_{s}}{N}} \begin{bmatrix} 0_{q\times 1} \\ \tilde{z}\left(k\frac{T_{s}}{N}\right) \end{bmatrix} - \int_{0}^{\frac{T_{s}}{N}} e^{\Lambda A_{m}\Lambda^{-1}\left(\frac{T_{s}}{N}-\tau\right)} \Lambda B_{m}\sigma\left(k\frac{T_{s}}{N}+\tau\right) d\tau.$$
(A34)

$$\zeta\left((k+1)\frac{T_{\rm s}}{N}\right) = e^{\Lambda A_{\rm m}\Lambda^{-1}\frac{T_{\rm s}}{N}} \begin{bmatrix} \overline{0}_{q\times 1} \\ \overline{z}\left(k\frac{T_{\rm s}}{N}\right) \end{bmatrix} - \int_0^{\frac{T_{\rm s}}{N}} e^{\Lambda A_{\rm m}\Lambda^{-1}\left(\frac{T_{\rm s}}{N}-\tau\right)} \Lambda B_{\rm m}\sigma\left(k\frac{T_{\rm s}}{N}+\tau\right) d\tau. \tag{A35}$$

Using (A12) and substituting the adaptive law from (22) and (65) for $\hat{\sigma}\left(k\frac{T_s}{N}\right)$ in (A34), we have

$$\chi\left((k+1)\frac{T_{\rm s}}{N}\right) = 0. \tag{A36}$$

From (A29), it follows that $\zeta(t)$ is the solution of the system:

$$\dot{\zeta}(t) = \Lambda A_{\rm m} \Lambda^{-1} \zeta(t) - \Lambda B_{\rm m} \sigma(t),$$

$$\zeta\left(k \frac{T_{\rm s}}{N}\right) = \begin{bmatrix} 0_{(n_{\rm m} - q) \times 1} \\ \tilde{z}\left(k \frac{T_{\rm s}}{N}\right) \end{bmatrix}, \quad t \in \left[k \frac{T_{\rm s}}{N}, (k+1) \frac{T_{\rm s}}{N}\right). \tag{A37}$$

Let

$$V(t) = \zeta^\top(t) \Lambda^{-\top} P \Lambda^{-1} \zeta(t), \quad \forall t \in \left[k \frac{T_{\rm s}}{N}, (k+1) \frac{T_{\rm s}}{N} \right).$$

Since Λ is nonsingular and P is positive definite, $\Lambda^{-\top}P\Lambda^{-1}$ is positive definite, and hence, V(t) is a positive-definite function. Using Lemma 3 and Equation (A37), it follows

$$V\left(\zeta\left(k\frac{T_{\rm s}}{N}\right)\right) = \tilde{z}^{\mathsf{T}}\left(k\frac{T_{\rm s}}{N}\right)\Lambda^{-\mathsf{T}}P\Lambda^{-1}\tilde{z}\left(k\frac{T_{\rm s}}{N}\right),\,$$

which, along with the upper bound in (A32), yields

$$V\left(\zeta\left(k\frac{T_{\rm s}}{N}\right)\right) \le \Delta_2(\bar{\gamma}_0). \tag{A38}$$

From (A37), it follows that, for all $t \in [k \frac{T_s}{N}, (k+1) \frac{T_s}{N})$,

$$\begin{split} \dot{V}(t) &= \zeta^{\mathsf{T}}(t) \Lambda^{-\mathsf{T}} P \Lambda^{-1} \Lambda A_{\mathsf{m}} \Lambda^{-1} \zeta(t) + \zeta^{\mathsf{T}}(t) \Lambda^{-\mathsf{T}} A_{\mathsf{m}}^{\mathsf{T}} \Lambda^{\mathsf{T}} \Lambda^{-\mathsf{T}} P^{\mathsf{T}} \Lambda^{-1} \zeta(t) - 2 \zeta^{\mathsf{T}}(t) \Lambda^{-\mathsf{T}} P \Lambda^{-1} \Lambda B_{\mathsf{m}} \sigma(t) \\ &= -\zeta^{\mathsf{T}}(t) \Lambda^{-\mathsf{T}} Q \Lambda^{-1} \zeta(t) - 2 \zeta^{\mathsf{T}}(t) \Lambda^{-\mathsf{T}} P \Lambda^{-1} \Lambda B_{\mathsf{m}} \sigma(t). \end{split}$$

Using the upper bound from (A23), for all $t \in \left[k\frac{T_s}{N}, (k+1)\frac{T_s}{N}\right]$, one can derive

$$\dot{V}(t) \le -\lambda_{\min}(\Lambda^{-\top}Q\Lambda^{-1}) \|\zeta(t)\|_{2}^{2} + 2\|\zeta(t)\|_{2} \|\Lambda^{-\top}PB_{m}\|_{2} \sqrt{q} \Delta_{1}(\bar{\gamma}_{0}). \tag{A39}$$

Notice that if

$$V(t) > \Delta_2(\bar{\gamma}_0), \quad \forall t \in \left[k\frac{T_s}{N}, (k+1)\frac{T_s}{N}\right),$$
 (A40)

the following holds:

$$\left\| \zeta(t) \right\|_2 > \sqrt{\frac{\Delta_2(\bar{\gamma}_0)}{\lambda_{\max}\left(\Lambda^{-\top}P\Lambda^{-1}\right)}} = \frac{2\sqrt{q}\Delta_1(\bar{\gamma}_0) \left\| \Lambda^{-\top}PB_{\mathrm{m}} \right\|_2}{\lambda_{\min}\left(\Lambda^{-\top}Q\Lambda^{-1}\right)}.$$

Moreover, the upper bound in (A39) yields

$$\dot{V}(t) < 0. \tag{A41}$$

From (A38), (A40), and (A41), it follows

$$V(t) \le \Delta_2(\bar{\gamma}_0), \quad \forall t \in \left[k\frac{T_s}{N}, (k+1)\frac{T_s}{N}\right),$$

and therefore

$$\zeta^{\top} \left((k+1) \frac{T_{s}}{N} \right) \Lambda^{-\top} P \Lambda^{-1} \zeta \left((k+1) \frac{T_{s}}{N} \right) \le \Delta_{2}(\bar{\gamma}_{0}). \tag{A42}$$

Then, (A33), (A36), and the upper bound in (A42) lead to the following inequality:

$$\tilde{\xi}^{\top} \left((k+1) \frac{T_{\rm s}}{N} \right) \Lambda^{-\top} P \Lambda^{-1} \tilde{\xi} \left((k+1) \frac{T_{\rm s}}{N} \right) \leq \Delta_2(\bar{\gamma}_0).$$

Using the result of Lemma 3, one can derive

$$\tilde{\boldsymbol{z}}^{\top} \left((k+1) \frac{T_{\mathrm{s}}}{N} \right) P_2 \tilde{\boldsymbol{z}} \left((k+1) \frac{T_{\mathrm{s}}}{N} \right) \leq \tilde{\boldsymbol{\xi}}^{\top} \left((k+1) \frac{T_{\mathrm{s}}}{N} \right) \Lambda^{-\top} P \Lambda^{-1} \tilde{\boldsymbol{\xi}} \left((k+1) \frac{T_{\mathrm{s}}}{N} \right) \leq \Delta_2(\bar{\gamma}_0),$$

which implies that the upper bound in (A32) holds for k + 1.

Next, from (A25), (A33), and (A36), it follows

$$\tilde{y}\left((k+1)\frac{T_{\rm s}}{N}\right) = \mathbf{1}_{n_{\rm m}q}^{\top}\zeta\left((k+1)\frac{T_{\rm s}}{N}\right),$$

and the definition of $\zeta\left((k+1)\frac{T_s}{N}\right)$ in (A35) leads to the following expression:

$$\tilde{y}\left((k+1)\frac{T_{\mathrm{s}}}{N}\right) = \mathbf{1}_{n_{\mathrm{m}}q}^{\mathsf{T}}e^{\Lambda A_{\mathrm{m}}\Lambda^{-1}\frac{T_{\mathrm{s}}}{N}} \left[\begin{array}{c} 0_{q\times 1} \\ \tilde{z}\left(k\frac{T_{\mathrm{s}}}{N}\right) \end{array}\right] - \mathbf{1}_{n_{\mathrm{m}}q}^{\mathsf{T}}\int_{0}^{\frac{T_{\mathrm{s}}}{N}}e^{\Lambda A_{\mathrm{m}}\Lambda^{-1}\left(\frac{T_{\mathrm{s}}}{N}-\tau\right)}\Lambda B_{\mathrm{m}}\sigma\left(k\frac{T_{\mathrm{s}}}{N}+\tau\right)d\tau.$$

The upper bounds in (A23) and (A32) yield the following upper bound:

$$\left\| \tilde{y} \left((k+1) \frac{T_{s}}{N} \right) \right\|_{2} \leq \left\| \eta_{2} \left(\frac{T_{s}}{N} \right) \right\|_{2} \left\| \tilde{z} \left(k \frac{T_{s}}{N} \right) \right\|_{2} + \int_{0}^{\frac{T_{s}}{N}} \left\| \mathbf{1}_{n_{m}q}^{\mathsf{T}} e^{\Lambda A_{m} \Lambda^{-1} \left(\frac{T_{s}}{N} - \tau \right)} \Lambda B_{m} \right\|_{2} \left\| \sigma \left(k \frac{T_{s}}{N} + \tau \right) \right\|_{2} d\tau \leq \varsigma(\bar{\gamma}_{0}, T_{s}),$$

where $\eta_2(\cdot)$, $\kappa(\cdot)$, and $\varsigma(\cdot, \cdot)$ are defined in (36), (37), and (44), respectively. This confirms the upper bound in (A31) for k+1. Hence, Equation (A30) holds for all $j\frac{T_s}{N} \le \tau_1$.

For all $j\frac{T_s}{N} + t \le \tau_1$, and $t \in \left[0, \frac{T_s}{N}\right]$, using the expression from (A26), we obtain

$$\tilde{y}\left(j\frac{T_{\mathrm{s}}}{N}+t\right) = \mathbf{1}_{n_{\mathrm{m}}q}^{\top}e^{\Lambda A_{\mathrm{m}}\Lambda^{-1}t}\tilde{\xi}\left(j\frac{T_{\mathrm{s}}}{N}\right) + \mathbf{1}_{n_{\mathrm{m}}q}^{\top}\int_{0}^{t}e^{\Lambda A_{\mathrm{m}}\Lambda^{-1}(t-\tau)}\Lambda\hat{\sigma}\left(j\frac{T_{\mathrm{s}}}{N}\right)d\tau - \mathbf{1}_{n_{\mathrm{m}}q}^{\top}\int_{0}^{t}e^{\Lambda A_{\mathrm{m}}\Lambda^{-1}(t-\tau)}\Lambda B_{\mathrm{m}}\sigma\left(j\frac{T_{\mathrm{s}}}{N}+\tau\right)d\tau.$$

The upper bound in (A23) and the expressions of $\eta_1(\cdot)$, $\eta_2(\cdot)$, $\eta_3(\cdot, \cdot)$, and $\eta_4(\cdot, \cdot)$, given in (36) and (42), lead to

$$\left\|\tilde{y}\left(j\frac{T_{\mathrm{s}}}{N}+t\right)\right\|_{2} \leq \|\eta_{1}(t)\|_{2}\left\|\tilde{y}\left(j\frac{T_{\mathrm{s}}}{N}\right)\right\|_{2} + \|\eta_{2}(t)\|_{2}\left\|\tilde{z}\left(j\frac{T_{\mathrm{s}}}{N}\right)\right\|_{2} + \eta_{3}\left(t,T_{\mathrm{s}}\right)\left\|\tilde{y}\left(j\frac{T_{\mathrm{s}}}{N}\right)\right\|_{2} + \eta_{4}(t)\sqrt{q}\Delta_{1}(\bar{\gamma}_{0}).$$

Consider (A30) and $\beta_1(\cdot)$, $\beta_2(\cdot)$, $\beta_3(\cdot)$, $\beta_4(\cdot)$ defined in (40)-(41). For arbitrary nonnegative integer j subject to $j\frac{T_s}{N} + t \le \tau_1$ and for all $t \in \left[0, \frac{T_s}{N}\right]$, we have

$$\left\| \tilde{y} \left(j \frac{T_{s}}{N} + t \right) \right\|_{2} \leq \beta_{1} \left(T_{s} \right) \varsigma(\bar{\gamma}_{0}, T_{s}) + \beta_{2} \left(T_{s} \right) \sqrt{\frac{\Delta_{2}(\bar{\gamma}_{0})}{\lambda_{\max} \left(P_{2} \right)}} + \beta_{3} \left(T_{s} \right) \varsigma(\bar{\gamma}_{0}, T_{s}) + \sqrt{q} \beta_{4} \left(T_{s} \right) \Delta_{1}(\bar{\gamma}_{0}).$$

Since the right-hand side coincides with the definition of $\gamma_0(\bar{\gamma}_0, T_s)$ in (45), we have the bound

$$\|\tilde{y}(t)\|_2 \le \gamma_0(T_{\rm s}, \bar{\epsilon}), \ \forall t \in [0, \tau_1],$$

which, along with the design constraint on T_s introduced in (54), yields

$$\|\tilde{y}_{\tau_1}\|_{\mathcal{L}_{\infty}} < \bar{\gamma}_0.$$

This clearly contradicts the statement in (A18). Therefore, $\|\tilde{y}\|_{\mathcal{L}_{\infty}} < \bar{\gamma}_0$, which proves (68). Furthermore, it follows from Lemma 5 that

$$\|e_t\|_{\mathcal{L}_{\infty}} < \Omega_1(T_s)\bar{\gamma}_0,$$

which holds uniformly for all $t \ge 0$ and therefore leads to the first upper bound in (69).

To prove the second bound in (69), from (3), (16), (56), (A4), (A5), and (A6), it follows

$$u_{\text{ref}}(s) - u(s) = C(s)P_{\text{m}}^{\text{n}}(s)\tilde{y}(s) - C(s)d_{\text{e}}(s) + (u_{\text{C}}(s) - u_{\text{M}}(s)) + (u_{\text{M}}(s) - u(s)), \tag{A43}$$

where $d_e(s)$ is the Laplace transform of $d_e(t)$ defined in (A7). In addition, u_C and u_M are defined in (A4) and (A5). Then, it leads to

$$\|u_{\text{ref}}(s) - u(s)\|_{\mathcal{L}_{\infty}} \le \|C(s)P_{\text{m}}^{-1}(s)\|_{\mathcal{L}_{1}} \|\tilde{y}\|_{\mathcal{L}_{\infty}} + \|u_{\text{C}}(s) - u_{\text{M}}(s)\|_{\mathcal{L}_{\infty}} + \|u_{\text{M}}(s) - u(s)\|_{\mathcal{L}_{\infty}} + \|C(s)\|_{\mathcal{L}_{1}} L_{\rho_{\text{I}}} \|e\|_{\mathcal{L}_{\infty}}. \tag{A44}$$

Combining (A14), (A15), (68), (69), and (A44) leads to

$$\|u_{\text{ref}}(s) - u(s)\|_{\mathcal{L}_{\infty}} < \Omega_2(T_s)\bar{\gamma}_0. \tag{A45}$$

This concludes the proof.

A.4 | Proof of Theorem 2

Using (4) and (11), the error $e_z(t)$ is governed by

$$\dot{e}_{z}(t) = A_{z}e_{z}(t) + B_{z}(r_{m}(t) - y(t)) - g(x(t), t), e_{z}(0) = 0.$$
(A46)

Then, we can rewrite (A46) as

$$\dot{e}_{z}(t) = A_{z}e_{z}(t) - (1 - \alpha)B_{z}W^{-1}\operatorname{sat}\left\{\frac{1}{1 - \alpha}WF_{z}e_{z}(t)\right\} + B_{z}\left(y_{\text{ref}}(t) - y(t)\right) + B_{z}\left(r_{F}(t) - y_{\text{ref}}(t)\right) + B_{z}\left(r_{m}(t) - r(t) + (1 - \alpha)W^{-1}\operatorname{sat}\left\{\frac{1}{1 - \alpha}WF_{z}e_{z}(t)\right\}\right) - g(x(t), t) + B_{z}\left(r(t) - r_{F}(t)\right).$$
(A47)

where the Laplace transforms of $r_{\rm F}(t)$ is given by

$$r_{\rm F}(s) = \frac{\mu}{s + \mu} r(s). \tag{A48}$$

Let

$$\mathcal{F}(t) = B_{z} \left(y_{\text{ref}}(t) - y(t) \right) + B_{z} \left(r_{\text{F}}(t) - y_{\text{ref}}(t) \right) + B_{z} \left(r_{\text{m}}(t) - r(t) \right) - g(x(t), t) + (1 - \alpha)B_{z}W^{-1} \text{sat} \left\{ \frac{1}{1 - \alpha}WF_{z}e_{z}(t) \right\} + B_{z} \left(r(t) - r_{\text{F}}(t) \right). \tag{A49}$$

Then, the equation in (A47) can be rewritten as

$$\dot{e}_{z}(t) = A_{z}e_{z}(t) - (1 - \alpha)B_{z}W^{-1} \operatorname{sat}\left\{\frac{1}{1 - \alpha}WF_{z}e_{z}(t)\right\} + \mathcal{F}(t). \tag{A50}$$

Select $V_z(t) = e_z^{\mathsf{T}}(t)Re_z(t)$ as the Lyapunov function for the closed-loop error dynamics in (A50). Then, the derivative of V_z can be obtained as

$$\dot{V}_{z}(t) = 2e_{z}^{\mathsf{T}}(t)R(A_{z}e_{z}(t) + \mathcal{F}(t)) - 2e_{z}^{\mathsf{T}}(t)RB_{z}(1-\alpha)W^{-1}\operatorname{sat}\left\{\frac{1}{1-\alpha}WF_{z}e_{z}(t)\right\}. \tag{A51}$$

We have $||e_z(0)||_{\infty} = 0 < \rho_z$. In addition, $e_z(t)$ is continuous. Therefore, if the bound in (60) is not true, there exists a time $\tau_1 > 0$ such that

$$||e_{z}(t)||_{\infty} < \rho_{z}, \quad \forall t \in [0, \tau_{1}), \quad ||e_{z}(\tau_{1})||_{\infty} = \rho_{z},$$

which implies that $\|e_{\mathbf{z}\tau_1}\|_{\mathcal{L}_{\infty}} = \rho_{\mathbf{z}}$. Then, by Lemma 6 and the condition in (49), we have for $\forall t \in [0, \tau_1]$ that

$$\dot{V}_{z}(t) \le \max_{i \in \{1, \dots, 2^q\}} \left\{ 2e_{z}^{\top}(t)R\left(A_{z}e_{z}(t) - B_{z}\left(D_{i}F_{z} + D_{i}^{\top}H_{z}\right)e_{z}(t) + \mathcal{F}(t)\right) \right\}. \tag{A52}$$

Furthermore, from the condition in (48), we obtain

$$\dot{V}_z(t) \le -e_z^{\top}(t)Se_z(t) + 2e_z^{\top}(t)R\mathcal{F}(t). \tag{A53}$$

Using the upper bound from (A53), for $t \in [0, \tau_1]$, one can derive

$$\dot{V}_{z}(t) \le -\lambda_{\min}(S) \|e_{z}(t)\|_{2}^{2} + 2\sqrt{p} \|e_{z}(t)\|_{2} \|R\|_{2} \|\mathcal{F}_{\tau_{1}}\|_{\mathcal{L}_{\infty}}. \tag{A54}$$

Notice that if

$$V_{z}(t) > \lambda_{\max}(R) \left(\frac{2\sqrt{p} \|R\|_{2} \|\mathcal{F}_{\tau_{1}}\|_{\mathcal{L}_{\infty}}}{\lambda_{\min}(S)} \right)^{2}, \tag{A55}$$

the following holds:

$$\|e_{\mathbf{z}}(t)\|_{2} > \frac{2\sqrt{p}\|R\|_{2}\|\mathcal{F}_{\tau_{1}}\|_{\mathcal{L}_{\infty}}}{\lambda_{\min}(S)}.$$
 (A56)

Moreover, the upper bound in (A54) yields

$$\dot{V}_{z}(t) < 0. \tag{A57}$$

From (A55)-(A57), it follows

$$V_{z}(t) \le \lambda_{\max}(R) \left(\frac{2\sqrt{p} \|R\|_{2} \|\mathcal{F}_{\tau_{1}}\|_{\mathcal{L}_{\infty}}}{\lambda_{\min}(S)} \right)^{2}, \tag{A58}$$

and therefore

$$\|e_{z_{r_1}}\|_{\mathcal{L}_{\infty}} \le \frac{2\sqrt{p}\|R\|_2 \|\mathcal{F}_{r_1}\|_{\mathcal{L}_{\infty}}}{\lambda_{\min}(S)}.$$
 (A59)

In the following, we obtain the bound on $\mathcal{F}(t)$ for $t \in [0, \tau_1]$. Using the result of the Theorem 1, it follows $||x||_{\mathcal{L}_{\infty}} < \rho_r + \bar{\gamma}_1$. Then, Assumption 1 implies that

$$\|g(x(t),t)\|_{\mathcal{L}_{\infty}} \le G_{\rho_r + \bar{\gamma}_1}. \tag{A60}$$

Moreover, from Theorem 1, one can obtain

$$\|y - y_{\text{ref}}\|_{\mathcal{L}} < \|C_x\|_{\infty} \Omega_1(T_s)\bar{\gamma}_0.$$
 (A61)

In addition, from (59) and (A48), we have

$$r_{\rm F}(s) - y_{\rm ref}(s) = \left(\frac{\mu}{s + \mu} \mathbb{I}_q - P_{\rm m}(s) K_{\rm g}\right) r(s) - C_{\rm m} \left(s \mathbb{I}_q - A_{\rm m}\right)^{-1} C_{\rm m}^{\dagger} y_0 - P_{\rm m}(s) \left(\mathbb{I}_q - C(s)\right) \sigma_{\rm ref}(s). \tag{A62}$$

It follows

$$\|r_{\mathrm{F}} - y_{\mathrm{ref}}\|_{\mathcal{L}_{\infty}} \leq \left\| \frac{\mu}{s + \mu} \mathbb{I}_{q} - P_{\mathrm{m}}(s) K_{\mathrm{g}} \right\|_{\mathcal{L}_{1}} M_{\mathrm{r}} + \left\| s C_{\mathrm{m}} \left(s \mathbb{I}_{q} - A_{\mathrm{m}} \right)^{-1} C_{\mathrm{m}}^{\dagger} C_{\mathrm{m}} \right\|_{\mathcal{L}_{\infty}} \rho_{0} + \left\| P_{\mathrm{m}}(s) \left(\mathbb{I}_{q} - C(s) \right) \right\|_{\mathcal{L}_{1}} \rho_{\Delta}. \tag{A63}$$

For all $t \in [kMT_s, (k+1)MT_s) \cap [0, \tau_1], \quad k \in \mathbb{Z}_{\geq 0}$, we obtain from (24) that

$$\left\| r_{\mathrm{m}}(t) - r(t) + (1 - \alpha)W^{-1}\operatorname{sat}\left\{\frac{1}{1 - \alpha}WFe_{z}(t)\right\}\right\|_{\infty} \leq \left\| (1 - \alpha)W^{-1}\left(\operatorname{sat}\left\{\frac{WF_{z}}{1 - \alpha}e_{z}(t)\right\} - \operatorname{sat}\left\{\frac{WF_{z}}{1 - \alpha}e_{z}(kMT_{s})\right\}\right)\right\|_{\infty} \\ \leq M_{r}\|WF_{z}\left(e_{z}(t) - e_{z}(kMT_{s})\right)\|_{\infty} \\ \leq M_{r}\|WF_{z}\|_{\infty}\|\left(e_{z}(t) - e_{z}(kMT_{s})\right)\|_{\infty}. \tag{A64}$$

From (A46), one can obtain

$$e_{z}(t) = e^{A_{z}(t - kMT_{s})}e_{z}(kMT_{s}) + \int_{kMT_{s}}^{t} e^{A_{z}(t - \tau)} \left(B_{z}\left(r_{m}(\tau) - y(\tau)\right) - g(x(\tau), \tau)\right) d\tau. \tag{A65}$$

Using Theorem 1, Lemma 4, and the bounds defined in (52), from (A60) and (A65), it follows

$$||e_{z}(t) - e_{z}(kMT_{s})||_{\infty} \le \gamma_{z}(\bar{\gamma}_{0}, T_{s}),$$
 (A66)

where $\gamma_z(\cdot, \cdot)$ is defined in (51). Let

$$r_{F_{-}}[k] = r_{F}(kMT_{s}), \ t \in [kMT_{s}, (k+1)MT_{s}), \quad k \in \mathbb{Z}_{>0}.$$
 (A67)

Then, from (A48) and (A67), we have

$$r_{F_{d}}[k] = \sum_{l=0}^{k} e^{-\mu l M T_{s}} (1 - e^{-\mu M T_{s}}) r_{d}[k - l].$$
(A68)

Using summation by part, it follows from (A68) that

$$r_{\mathrm{F_d}}[k] = r_{\mathrm{d}}[k] + \sum_{l=0}^{k} e^{-\mu(l+1)MT_{\mathrm{s}}} (r_{\mathrm{d}}[k+1-l] - r_{\mathrm{d}}[k-l]). \tag{A69}$$

Then, one can obtain

$$||r_{F_d}[k] - r_d[k]||_{\infty} \le \sum_{l=0}^k e^{-\mu(l+1)MT_s} ||r_d[k+1-l] - r_d[k-l]||_{\infty}.$$
(A70)

From (14), (24), (A64), and (A66), for any $k \in \mathbb{Z}_{\geq 0}$, we have

$$||r_{d}[k+1] - r_{d}[k]||_{\infty} \le M_{r}||WF_{z}||_{\infty}\gamma_{z}(\bar{\gamma}_{0}, T_{s}) + MT_{s}\delta_{r} . \tag{A71}$$

From (A70) and (A71), it follows

$$||r_{F_d}[k] - r_d[k]||_{\infty} \le \frac{e^{-\mu M T_s}}{1 - e^{-\mu M T_s}} \left(M_r ||WF_z||_{\infty} \gamma_z(\bar{\gamma}_0, T_s) + M T_s \delta_{r_m} \right). \tag{A72}$$

Taking the discretization error into account, we have

$$||r_{\rm F} - r||_{\mathcal{L}_{\infty}} \le \frac{e^{-\mu M T_{\rm s}}}{1 - e^{-\mu M T_{\rm s}}} \left(M_{\rm r} ||W F_{\rm z}||_{\infty} \gamma_{\rm z}(\bar{\gamma}_0, T_{\rm s}) + M T_{\rm s} \delta_{\rm r_m} \right) + 2 \left(1 - e^{-\mu M T_{\rm s}} \right) M_{\rm r}. \tag{A73}$$

Then, from (A60)-(A73), it follows

$$\begin{split} \|\mathcal{F}\|_{\mathcal{L}_{\infty}} &\leq \|B_{z}\|_{\infty} \|P_{m}(s)(\mathbb{I}_{q} - C(s))\|_{\mathcal{L}_{1}} \rho_{\Delta} + \|B_{z}\|_{\infty} \|C_{x}\|_{\infty} \Omega_{1}(T_{s})\bar{\gamma}_{0} + \gamma_{r}(\bar{\gamma}_{0}, T_{s}) + G_{\rho_{r} + \bar{\gamma}_{1}} \\ &+ \|B_{z}\|_{\infty} \left\| \frac{\mu}{s + \mu} \mathbb{I}_{q} - P_{m}(s)K_{g} \right\|_{\mathcal{L}_{1}} M_{r} + \|B_{z}\|_{\infty} \left\| sC_{m} \left(s\mathbb{I}_{q} - A_{m} \right)^{-1} C_{m}^{\dagger} C_{m} \right\|_{\mathcal{L}_{1}} \rho_{0} \\ &+ \frac{1}{\mu} \|B_{z}\|_{\infty} \left(\frac{1}{MT_{s}} M_{r} \|WF_{z}\|_{\infty} \gamma_{z}(\bar{\gamma}_{0}, T_{s}) + \delta_{r_{m}} \right). \end{split}$$
(A74)

Since $T_{\rm s} \leq T_{\rm s_{\rm max}}$ is selected such that the inequalities in (54) hold, we have $\gamma_{\rm r}(\bar{\gamma}_0,\,T_{\rm s}) < \bar{\gamma}_{\rm r}$. Therefore,

$$\left\| \mathcal{F}_{\tau_1} \right\|_{\mathcal{L}_{\infty}} < \left(1 - \frac{2\sqrt{p} \|R\|_2 \Delta_{\mathbf{s}}(\mu, F_{\mathbf{z}})}{\lambda_{\min}(S)} \right)^{-1} \Delta_{\mathcal{F}}(\mu, F_{\mathbf{z}}), \tag{A75}$$

where $\Delta_s(\mu, F_z)$ and $\Delta_F(\mu, F_z)$ are defined in (46). From (A59) and (A75), it follows

$$\left\| e_{\mathbf{z}_{\mathbf{r}_{\mathbf{l}}}} \right\|_{\mathcal{L}_{\infty}} < \rho_{\mathbf{z}},\tag{A76}$$

which contradicts with $\|e_{z_{\tau_1}}\|_{\mathcal{L}_{\infty}}=\rho_z$. Hence, the inequality in (71) is true.